



SCIENCE OF
TSUNAMI HAZARDS

The International Journal of The Tsunami Society

Volume 12 Number 1

1994

- NUMERICAL SIMULATION OF 1969 TSUNAMI ALONG THE PORTUGUESE COASTS. PRELIMINARY RESULTS** **3**
 PH. HEINRICH
 Commissariat a l' Energie Atomique, Bruyeres-le-Chatel, France
 M. A. BAPTISTA, P. MIRANDA
 Universidade de Lisboa, Lisboa, Portugal
- ON THE INFULENCE OF THE SIGN OF THE LEADING TSUNAMI WAVE ON THE HEIGHT OF RUN-UP ON THE COAST** **25**
 S. L. SOLOVIEV
 Academy of Science, Moscow, Russia
 R. Kh. MAZOVA
 Novgorod State Technical University, Nizhy Novgorod, Russia
- MODELING THE 105 Ka LANAI TSUNAMI** **33**
 CARL JOHNSON
 University of Hawaii, Hilo, Hawaii USA
 CHARLES L. MADER
 University of Hawaii, Honolulu, Hawaii USA
- THE T-PHASE OF THE 1 APRIL 1946 ALEUTIAN ISLANDS TSUNAMI EARTHQUAKE** **39**
 DANIEL A. WALKER
 University of Hawaii, Honolulu, Hawaii USA
 PAUL G. OKUBO
 Hawaiian Volcano Observatory, Hawaii USA
- EFFECT OF THE NEXT DATA POINT ON TSUNAMI FLOOD LEVEL PREDICTION** **53**
 FRED E. CAMFIELD AND DEBRA R. GREEN
 Coastal Engineering Research Center, Vicksburg, Mississippi USA
- MEMORIUM - PROFESSOR SERGEI SOLOVIEV** **60**

OBJECTIVE: The **Tsunami Society** publishes this journal to increase and disseminate knowledge about tsunamis and their hazards.

DISCLAIMER: Although these articles have been technically reviewed by peers, **The Tsunami Society** is not responsible for the veracity of any statement, opinion or consequences.

EDITORIAL STAFF

Dr. Charles L. Mader, Editor

JTRE-JIMAR Tsunami Research Effort, University of Hawaii
1000 Pope Rd., MSB-312, Honolulu, HI. 96822, USA

Dr. Augustine S. Furumoto, Publisher

Mr. George D. Curtis, Production

EDITORIAL BOARD

Professor George Carrier, Harvard University

Dr. Zygmunt Kowalik, University of Alaska

Dr. Shigehisa Nakamura, Kyoto University

Dr. Yurii Shokin, Novosibirsk

Mr. Thomas Sokolowski, Alaska Tsunami Warning Center

Dr. Costas Synolakis, University of California

Professor Stefano Tinti, University of Bologna

TSUNAMI SOCIETY OFFICERS

Dr. Fred Camfield, President

Professor Stefano Tinti, Vice President

Commander Dennis Sigrist, Secretary

Dr. Augustine Furumoto, Treasurer

Mr. George Curtis, Director

Submit manuscripts of articles, notes or letters to the Editor. If an article is accepted for publication the author(s) must submit a camera ready manuscript in the journal format. A voluntary \$50.00 page charge (\$25.00 for Tsunami Society Members) will include 50 reprints.

SUBSCRIPTION INFORMATION: Price per copy \$20.00 USA

ISSN 0736-5306

Published by **The Tsunami Society** in Honolulu, Hawaii, USA

NUMERICAL SIMULATION OF THE 1969 TSUNAMI ALONG THE PORTUGUESE COASTS. PRELIMINARY RESULTS.

Ph Heinrich

Laboratoire de Détection et de Géophysique

Commissariat à l'Energie Atomique, Bruyères-le-Châtel, France

M. A. Baptista , P. Miranda

Centro de Geofisica da Universidade de Lisboa

Lisboa, Portugal

ABSTRACT

On the 28th February 1969, the coasts of Portugal, Spain and Morocco were affected by water waves generated by a submarine earthquake ($M_s=7.9$) with epicenter located south of the Gorringe bank. The aim of this paper is to simulate this small tsunami, by comparing the computed and observed tide gauges. According to Fukao, the fault plane solution is a thrust with a small strike slip component $N55^\circ E$ parallel to the Gorringe Bank, the soil movement area involved being $80 \times 50 \text{ km}^2$. Nonlinear shallow water equations are solved with a finite difference scheme, using a computational grid with different cell sizes over different geographical domains. The water surface initialisation has been computed from Okada's formulas, which output ground deformation as a function of seismic parameters. The numerical results show that a great part of the tsunami energy is refracted towards the Portuguese coasts. The modelled waves compare well with the recorded waves in respect to travel times, maximum amplitudes and periods. Other possible source locations, as well as other fault plane selections have been studied.

INTRODUCTION

At 2h 40mn 32s a.m. on the 28th February 1969, an earthquake with magnitude $M_s=7.9$ occurred south of the Gorringe Bank. This seismic event is one of the largest that affected this area. The most famous one occurred in 1755 and killed probably more than 50,000 persons (directly and through the induced tsunami).

The 1969 earthquake generated a small tsunami recorded by most of the tide stations of Portugal mainland, Spain and of the Azores islands. The analysis of the gauge records was carried out by M. A. Baptista et al. (1992). Spectral analysis allowed them to filter the tide, and to determine the main characteristics of the signals such as the tsunami arrival times, the maximum amplitudes and the tsunami periods. Comparing "quiet days" records and "tsunami-days" records, they concluded that the frequencies recorded on a particular spot are connected to the local bathymetry and that the occurrence of the tsunami increases the amplitude of only one frequency in the spectrum. Inverse ray-tracing from different coastal stations allowed them to determine the tsunami source close to the Gorringe Bank.

The aim of this paper is to simulate the recorded water waves by means of numerical models. First, the seismic source is briefly described and the ground displacement is determined from Okada's (1985) formulas, using Fukao's (1973) seismic parameters. The water waves propagation is then computed using shallow water models or three-dimensional Navier-Stokes models. Finally, other tsunami sources are studied for this event.

DESCRIPTION OF THE SEISMIC SOURCE

The fracture zone extending from the Azores towards the Strait of Gibraltar is the boundary between the Eurasian and African tectonic plates. The analysis of the earthquake focal mechanisms in this zone (Fig.1) shows that the relative motion between the two plates changes from right lateral strike slip with an extensional component at the western end, to pure strike slip in the central area and thrusting with a compressive component in the NW direction at the eastern end. This behaviour can be explained in terms of a pole of rotation for the relative motion of the two plates (cf Minster, 1978; Buforn, 1988). According to Purdy (1975), the 1969 shock is a direct consequence of the compressive motion in the eastern end of the zone, with underthrusting of the African plate at an extremely low rate. The seismic-refraction lines of this area as well as the free-air gravity anomaly over the Gorringe Bank allow him to conclude that the Gorringe ridge was formed as a continuous process by the successive overthrusting of oceanic crustal and upper mantle material.

The 1969 earthquake epicenter was located by different seismic organizations at N36.01 W10.6(USGS), N36.2 W10.5 (BCIS) and N36.1 W10.8 (LCSSM). The epicenter as well as the aftershock area are located in the Eastern Horseshoe Abyssal Plain, south of the Gorringe Bank. (Fig. 2). According to seismologists, the focal mechanism is a thrust faulting with a small strike slip component. The problem is to distinguish between the fault plane and the auxiliary plane. Lopez et al. (1972), Udias et al. (1976), Buforn et al. (1988) favor the selection of the east-west striking plane, whereas McKenzie (1970), Fukao (1973), Purdy (1975) choose the N55°E striking fault, parallel to the Gorringe Bank.

According to Fukao, the elongation in the NE-SW direction of the aftershock area suggests that the fault strike angle is N55°E. The length and the width of the fault are estimated from the aftershock area to be about L=80km and W=50km respectively. From seismic signals analysis, the dip angle is estimated to be 52° and the seismic moment $M_0=6.10^{20}$ N.m. On the basis of this analysis, it has been decided to simulate first the tsunami generated by this fault plane. The slip dislocation u has been calculated from the following formula, based on shear faulting theory :

$$M_0 = \mu u L W$$

where μ is the shear modulus of the surrounding rocks. In this case, if we assume $\mu=4.10^{10}$ N/m² (cf Fukao, 1973), the slip dislocation is about 4 meters. This slip is consistent with those presented by Scholz (1982) for a thrust event, taking into account a fault length of 80 km.

In order to calculate the ground deformation from these fault parameters, Okada's (1985) formulas have been computed. These formulas have been established by Okada assuming an elastic, isotropic and homogeneous half space. They calculate the ground displacement as a function of seismic parameters (the dip angle, the strike angle, the fault length and fault width, the depth of the upper edge of the fault and the slip dislocation) and of the surrounding rocks parameters (the Lamé's coefficients λ and μ). Figure 3 shows the vertical computed sea-floor displacement, using the Fukao's seismic parameters. The dimensions of the subsidence areas are greater than the uplift area dimensions, but the maximum subsidence height at the rupture front is about four times lower than the maximum uplift height.

TSUNAMI PROPAGATION MODELS

Most simulations of tsunami propagation have been carried out using a shallow water model. In order to assess the importance of the frequency dispersion, the results for one of the simulations have been compared with those obtained by solving the three-dimensional Navier-Stokes equations.

The shallow water model :

This model, adapted from the SWAN model (Mader, 1988) solves nonlinear long wave equations, using an explicit-in-time finite difference scheme with C-type grids. The equations are formulated either in cartesian coordinates or in spherical coordinates. The latter coordinates have been used to propagate tsunamis over long distances (from the source to the Azores islands and to the Canaries islands). The cartesian coordinates system has been preferred for the propagation from the source to Portugal and Spain mainlands, because Okada's (1985) formulas and some local bathymetries are available only in cartesian coordinates.

The first simulation presented in this paper has been achieved using coarse grids with cell sizes of $1 \times 1 \text{ km}^2$. In order to propagate tsunamis in shallow water regions with more than ten points per wavelength, coupling between coarse and fine grids has been used in coastal regions. Wave heights and velocities along the boundaries of the fine grid are interpolated spatially from the coarse grid values at each time step. Fine grid values are not used as input of the coarse grid, since it is assumed that waves reflected by the coasts in the fine grid are not significantly different from reflected waves in the coarse grids.

At the shoreline, the velocities are set in this case to zero, so that complete reflection is computed. This assumption overestimates the computed water waves amplitudes, since no wave dissipation by run-up occurs. At the open ocean boundaries, one-dimensional radiation conditions are computed for each axis separately.

The Navier-Stokes model :

The 3D hydrodynamics program Nasa-Vof3D (developed by Torey et al. in 1987) has been modified in order to study earthquake-induced or landslide-generated tsunamis (cf Heinrich, 1992). This eulerian model solves the three-dimensional incompressible Navier-Stokes equations with a free-surface. The modifications consisted in dealing with any three-dimensional time-dependent bathymetry and in introducing the possibility of rezoning in shallow water regions. The rezoning consists in stopping the calculation in the coarse grid at a selected instant and in pursuing it in a fine grid. The connection between these two grids is carried out by initiating only once the velocities and water heights of the fine grid from the coarse grid values. The main disadvantage of this method is to propagate in the fine grid only the first waves of the tsunami.

The meshes used in the simulation consist of about $150 \times 150 \times 20$ cells in the x, y, z directions respectively with variable spacings ranging from 5km to 1km in the horizontal directions.

Computed source :

Compared with the tsunami celerity (0.2km/s), the rupture velocity (about 3km/s) is large, so the ground displacement over the whole faulting region is assumed to be instantaneous. The origin time $t=0s$ is chosen at this instant. Since the source dimensions are much larger than the water depth, the water surface elevation is given by the vertical motion of the bottom. Figure 3 shows then also the initialisation of the water surface for a N55°E orientation of the fault.

Propagation :

For both models, the Coriolis and frictional effects were neglected. As regards shallow water simulations, the nonlinear terms are negligible. The wave elevations computed at the coastal stations are almost similar, when linearizing the governing equations. From this result, it can be inferred that the modelled waves amplitudes are directly proportional to the ground slip dislocation.

COMPARISONS BETWEEN THE COMPUTED AND RECORDED WAVES

The best agreement between computed and recorded waves has been found for a hydraulic source centered approximately at the earthquake epicenter (defined by USGS data) with a N55°E strike angle.

The results of two calculations are presented in this paragraph. The first simulation uses cells of 1x1 km² and propagates waves from the source to Portugal and Spain mainlands. The propagation over long distances (up to the Azores Islands and the Canaries) has been simulated in the spherical coordinates system, using cells of 1.5 minute.

The computed water surfaces at $t=1000s$, $t=2000s$, $t=3000s$ and $t=5000s$ are shown in Figs. 4, 5 and 6. As seen at $t=1000s$, the directivity of the waves energy is quite important, most of the energy propagates perpendicular to the fault orientation (cf Ward, 1980). Later, as waves are refracted along the south and west Portuguese coasts, the energy directivity is attenuated. At all the coastal stations, the first wave motion is small and negative, since large subsidence areas are located north and south of the uplifted area. Offshore, waves are strongly refracted and reflected by the Gorringe Bank. The two sea-mounts forming the Gorringe Bank, are acting as secondary sources. As shown in Fig. 5 at $t=3000s$, waves reaching the west Portuguese coast are originating from the Gorringe Bank and not from the earthquake epicenter. At one hour and a half after the origin time, waves reflected by the Moroccan coasts reach the south Portuguese and Spanish coasts (Fig. 6). These reflection phenomena accounts for the high wave amplitudes that have been recorded for more than 6 hours along these coasts.

With the resolution used in simulations, it is not possible to match exactly the location of the tide gauges in Portugal, in Spain or in the Azores. Numerical simulations revealed minor

differences in waveforms at cells located side by side. We therefore have chosen the cells with the most representative depth values, i.e. depths of about 5 meters for most of the gauges. Figures 7, 8 and 9 show comparisons between computed and recorded waves at Lagos, Faro, Cadiz, Cascais, Horta (Azores Islands), Pedrouços and Cacilhas. The latter two tide gauges are located in the Tagus Estuary.

At **Lagos**, the modelled waves at a 4 meters depth match well the recorded waves in respect to the travel times, the periods and the wave amplitudes. The period of the first modelled crest is slightly longer than the recorded one. The same first waves are obtained in coupling a coarse grid with a fine grid with cells of $250 \times 250 \text{m}^2$. The disagreement about the leading wave period could be explained by an overestimation of the source dimensions.

Faro is located approximately 60 km eastward of Lagos in a small river, which goes through a very shallow water bay, closed by dunes. The precise bathymetry in this area as well as the tide gauge location are not well represented, so that the river and the sand islands have not been taken into account in the model. The modelled waves reach Lagos and Faro simultaneously at 2000 seconds, since the first waves of the tsunami are refracted by the coasts and are propagating in a perpendicular direction to the shoreline (Fig. 5). Except for the time difference of about six minutes, the first modelled waveforms are similar to the recorded ones.

The **Cadiz** harbour is located at the mouth of a large river. The first computed wave gauge (Fig. 7) is located at a 13 meters depth at the mouth of the river, the second one is computed 3 km inside the river at a 7 meters depth. The comparison with the recorded waves shows that the second computed wave gauge is probably closer to the tide gauge. Only the first wave is well reproduced. The periods of the following recorded waves (about 17 minutes) are longer than the leading wave period, being about two times longer than the modelled ones. These low frequencies are likely to be generated by resonance in the river or in the Cadiz bay. The imprecisions of the bathymetry could account for these discrepancies.

At **Cascais**, important discrepancies between the recorded and the computed waves are observed in Fig.8. The waveforms from $t=2000$ seconds to $t=3500$ s are completely different from one another. Only the arrival time of the wave train seems to be accurate, since the maximum amplitude of the first computed trough is observed at $t=2300$ s in the simulation as well as on the record. Later, the correlation between the two signals is improving, as far as wave shapes are concerned. The amplitudes of the first four waves are too large by about a factor of three, whereas the wave amplitudes are on the same order as the recorded ones from $t=4500$ s to $t=8000$ s. These discrepancies could be attributed either to an incorrect response of the tide gauge to this tsunami, or to inaccurate simulation. These points are discussed in the next paragraphs.

In the Tagus estuary, the locations of the tide gauges are **Pedrouços**, **T. Paço**, and **Cacilhas** (Fig. 8). Since the Tagus river is narrow, waves entering in the Tagus propagate

eastward in a one-dimensional way. This result is confirmed by the similarity between the signals recorded at Pedrouços, Cacilhas and T. Paço. As T. Paço is located 2km north of Cacilhas, the signals are nearly identical and so the T. Paço tide gauge is not represented.

As shown in Fig. 8 at Pedrouços, excellent agreement is found between the simulations and the observations. The period, the amplitude and the travel time of each individual modelled wave agree very closely with the recorded ones. At $t=4000s$ (Fig. 6) the first two crests reaching Cascais have joined at the Tagus mouth and are forming only one crest with a half-period of about 500 seconds and a 0.4 meters amplitude. This wave propagates eastward with slight deformation up to Cacilhas and is well reproduced by the model. The discrepancies concerning the following waves at Cacilhas are due to poor grid resolution.

At Horta, the agreement between the recorded and computed waves is satisfactory. The first modelled gauge (Fig. 9) is located at a 5 meters depth, and the second at a 70 meters depth. The results at a 70 meters depth show that the water surface elevation offshore does not exceed 5 centimeters. Wave shoaling and wave reflections by the Azores islands account for the 20cms recorded at Horta. Only the two first waves are well reproduced by the numerical model. The third one is preceded by very short small waves that are likely to be due to wave reflection and that are not modelled.

Fig. 9 shows the numerical results at Casablanca (Morocco) and at Santa Cruz (Canaries Islands), where waves with amplitudes of 1.20m and 0.20m respectively have been reported (cf Lopez et al., 1972). At Casablanca, the maximum amplitude of the computed waves is about 2 meters at a 5 meters depth. These high amplitudes are accounted for by the source directivity (Fig. 4) and by wave shoaling. Unfortunately records from Morocco, which would have been very important for confirming the source parameters, are not available.

The Canaries are volcanic islands with very steep slopes, located at about 1000km from the source. As expected, the first computed wave heights are small in agreement with the observations.

NUMERICAL RESULTS AT CASCAIS

The numerical results at Cascais are in poor agreement with the observations, whereas the results in the Tagus estuary at 15km and 25km away from Cascais are satisfactory. The spectra of the recorded and computed signals at Cascais have been calculated for a time interval of 8000s (fig. 10). As shown in this figure, the observed peaks are ranging from 5 to 20 minutes and are approximately reproduced by the model. The discrepancies observed in the previous paragraph could be accounted for by a poor response of the tide gauge to short periods (cf Satake et al., 1988).

In order to check the model validity, other numerical simulations have been performed. The 3D Navier-Stokes model has been used to estimate the frequency dispersion. This 3D simulation has been carried out by rezoning a 600x600 km² computed domain at t=1500 seconds. In this domain, the cell sizes are about 3x3 km² in the horizontal directions. In the second domain, the cell sizes are about 1x1 km² in the Cascais area. The comparison between the two numerical models (Fig. 10) shows that the results are similar for the first waves and so that the effects of frequency dispersion on computed waves at Cascais are only minor. This result was expected, since the number of wave lengths from the source to Cascais is small. The differences observed in Fig. 10 are attributed mainly to the differences between the two gauge locations.

As regards shallow water simulations, it was noticed that results in the previous paragraph are slightly different for cells located side by side. In order to propagate the waves with smaller cells, a second grid covering the Cascais area has been used with 250x250m² cells. This fine grid with 300x300 cells is coupled with the previous coarse grid (the cells sizes of this latter grid are 1x1 km²). Fig. 10 shows that the wave trains are roughly comparable.

From these results, it can be inferred that the numerical model is likely not to be responsible for the disagreements between the first computed and observed waves at Cascais. Other potential tsunami sources are then studied in the next paragraphs.

NUMERICAL RESULTS OBTAINED WITH DIFFERENT STRIKE ANGLES

In this paragraph, new simulations have been carried out, selecting other fault planes. Since the fault plane could be mistaken for the auxiliary plane, the east-west fault plane has been first selected. Taking into account the focal mechanism, it is then assumed that the south block is moving upward in respect to the north block. The strike angle is 270° in respect to the North, the other seismic parameters are unchanged.

Fig. 11 shows the comparisons between the recorded and the N55°E and 270° modelled waves at Lagos, Cascais and Pedrouços. At Lagos, the 270° modelled waves are very similar to the previous modelled waves. The wave refraction towards the coasts is such, that no significant difference is observed.

Due to the location of the uplifted area, the modelled waves arrive at Cascais and Pedrouços four minutes later than the N55°E modelled waves. At Cascais, the amplitudes of the first crest and of the third trough are about 75 cms, two times higher than the previous modelled amplitudes. At Pedrouços, the amplitude differences between the two modelled waves are reduced to about 20cms. Only, the source directivity can account for these high amplitudes.

The same calculations have been carried out, using a 25° strike angle corresponding approximately to the Messejana fault and a 90° strike angle. The numerical results show that the fault direction has minor effects on waveforms and on wave periods. Only the waves amplitudes vary significantly with the the fault direction. These results are in fair agreement with Ward's (1980) formulas, that scale the waveforms for a dip slip earthquake by $\sin\phi$, where ϕ is the azimuth of observation in respect to the fault direction. The comparisons between recorded and all the computed wave heights suggest that the $N55^\circ E$ fault plane is the best choice.

NUMERICAL RESULTS OBTAINED WITH A DIFFERENT SOURCE LOCATION

As mentioned above, the earthquake epicenter has been located by most of the seismologists within 30 km of the U.S.G.S. epicenter. In this paragraph, the source location has been chosen 60 km north-west with respect to the previous one, assuming that the Gorringe Bank has been uplifted by this event. This hypothesis is in agreement with the theories of Purdy (1975) or Minster (1978). It is also worth noting that the Gorringe Bank dimensions (about $100 \times 50 \text{ km}^2$) are approximately the same as the uplifted ground dimensions of Figure 3.

The numerical results at Lagos, Cascais and Pedrouços are shown in Fig. 12. The waves arriving at Lagos are similar to the modelled waves of the first simulation in respect to the periods and to the amplitudes. The only difference is that the modelled waves lag the observations by about 5 minutes. The same time difference is observed at Faro and Cadiz. At Cascais and Pedrouços, waves arrive about 5 minutes sooner than the recorded waves. The amplitudes of the first waves at Cascais (about 50 cms) are slightly greater than the amplitudes of the modelled waves of the first simulation. The first two crests, computed in the first numerical simulation, are replaced by only one crest with half-period of 10 minutes. This crest is followed by a 0.50cm high trough with about the same half-period. This large trough is then propagating in the Tagus estuary, as shown on the modelled Pedrouços gauge. The second recorded crest at Pedrouços at 4100s is not reproduced.

The comparisons between the two numerical simulations show that the location of the source in respect to the Gorringe bank is important and that a great part of energy is reflected by the two sea-mounts, when locating the source south of the Gorringe Bank. These results suggest that the seismic location is probably close to the real one. The location will be confirmed in a second report, taking into account a more precise bathymetry offshore and close to the tide gauge stations.

CONCLUSION

The numerical simulation of the 1969 Portuguese tsunami has been performed, using different sources and different models. For each case, comparisons between the recorded and computed wave gauges have been made.

Fair agreement has been obtained for most of the eight studied gauges, using the Fukao's (1973) seismic parameters. The exception is the Cascais gauge, where the first recorded waves are not reproduced by the models. Since the results at Cascais are not very sensitive to the source, the discrepancies could be attributed either to the tide gauge response to tsunamis or to a local complex bathymetry, which the model probably does not take into account. The 26th May 1975 earthquake generated also a small tsunami recorded by most of the tide gauge stations. This study will allow us to determine, if the Cascais records can be modelled.

The magnitude of the 1755 tsunami, which epicenter is maybe close to the 1969 one, was estimated to be about 8.5-9, whereas the observed wave amplitudes at Lisbon and Cadiz were 10 to 20 times higher than those recorded in 1969. The numerical simulation of the 1755 tsunami will then require particular attention to the propagation of strong nonlinear waves, to bores formation and to tsunami runup.

ACKNOWLEDGMENTS

The authors are grateful to Drs Ribeiro A. and Avouac J. Ph. for their suggestions about the source and to Dr. Roche R. for the useful discussions about numerical simulations. This work has been carried out within the framework of the G.I.T.E.C. project (Genesis and Impact of Tsunamis on the European Coasts). The GITEC contract has been undertaken for the Commission of the European Communities under the Directorate General for Science, Research and Development.

REFERENCES

BAPTISTA M. A., MIRANDA P., MENDES VICTOR L., 1992. Maximum entropy analysis of Portuguese tsunami data, the tsunamis of 28.02.1969 and 26.05.75. *Science of Tsunami Hazards*, vol. 10, n°1.

BUFORN E., UDIAS A, COLOMBAS M. A., 1988. Seismicity, source mechanisms and tectonics of the Azores-Gibraltar plate boundary. *Tectonophysics*, 152, pp 89-118.

- FUKAO, 1973. Thrust faulting at a lithospheric plate boundary, the Portugal earthquake of 1969. *Earth and Planetary Science Letters* 18, pp 205-216.
- HEINRICH, P., 1992. Nonlinear water waves generated by landslides. *Journal of Waterways, Port, Coastal and Ocean Engineering, A.S.C.E.* , Vol. 118, n°3, pp 249-266, May/June.
- LOPEZ ARROYO A., UDIAS A., 1972. Aftershock sequence and focal parameters of February 28, 1969 earthquake of the Azore-Gibraltar zone. *Bull. of the Seismological Society of America*, vol 62, pp 699-720 , June.
- MADER C. L., 1988. *Numerical Modeling of Water Waves*, University of California Press, Berkeley, California.
- MCKENZIE D. P., 1970. Plate tectonics of the Mediterranean region. *Nature*, 226, pp 239-243.
- MINSTER J. B., JORDAN T. H., 1978. Present day plate motions. *J. Geophys. Res.*, 83, pp 5331-5354.
- OKADA Y., 1985. Surface deformation due to shear and tensile faults in a half space. *Bull of the Seismological Society of America*, 75, n° 4, pp 1135-1154, August.
- PURDY G. M., 1975. The Eastern End of the Azores-Gibraltar Plate Boundary. *Geophys. J. R. Astr. Soc.*, 43, pp 973-1000.
- SATAKE K., OKADA M., ABE K., 1988. Tide gauge response to tsunamis : Measurements at 40 tide gauge stations in Japan. *J. Marine Res.*, 46, pp 557-571.
- SCHOLZ C. H., 1982. Scaling laws for large earthquakes : consequences for physical models. *Bull. of the Seismological Society of America*, Vol. 72, n° 1, pp 1-14., Feb.
- TORREY, M. D. et al. , 1987. Nasa-Vof3D : a three-dimensional computer program for incompressible flows with free surfaces. Los Alamos National Laboratory Report, LA-11009-MS.
- UDIAS A., LOPEZ ARROYO A., MEZCUA J., 1976. Seismotectonic of the Azores-Alboran region. *Tectonophysics*, 31, pp 259-289.
- WARD S. N., 1980. Relationships of tsunami generation and an earthquake source. *J. Phys. Earth*, 28, pp 441-474.

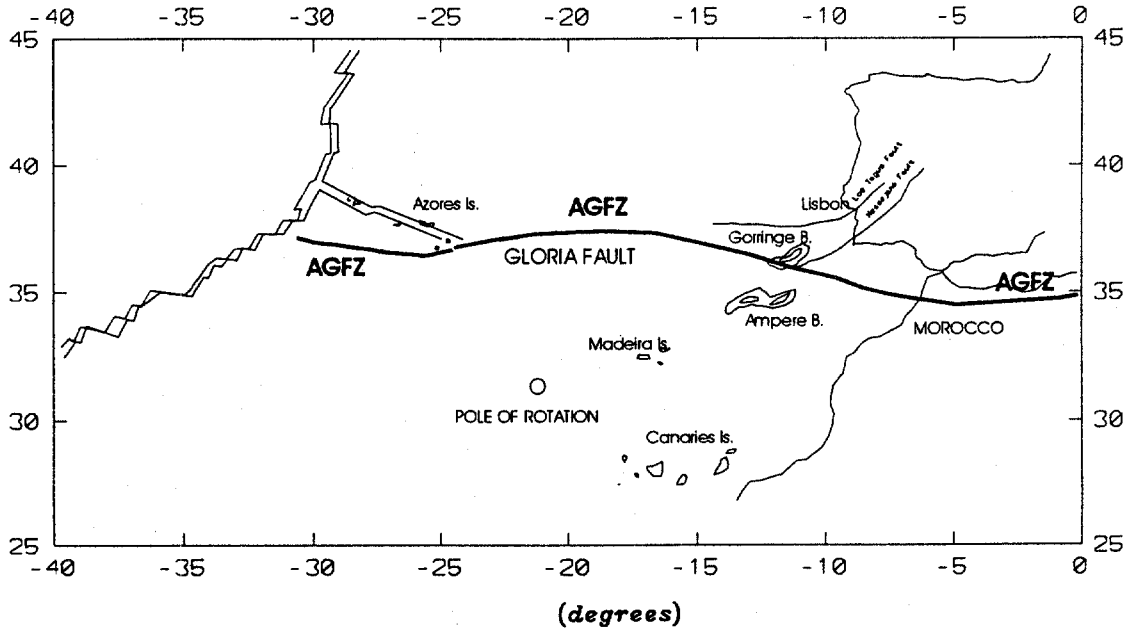


Figure 1. Location of the Azores-Gibraltar Fracture Zone (AGFZ)

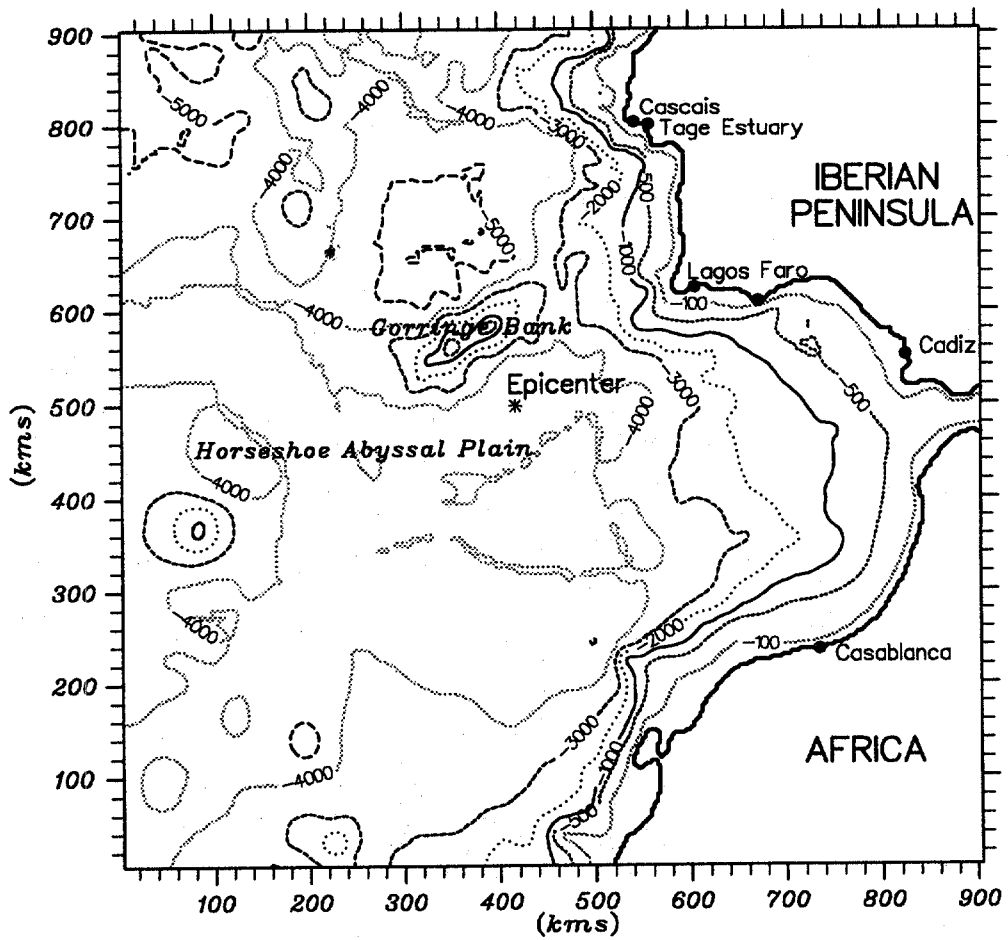


Figure 2. Bathymetry used for numerical simulations

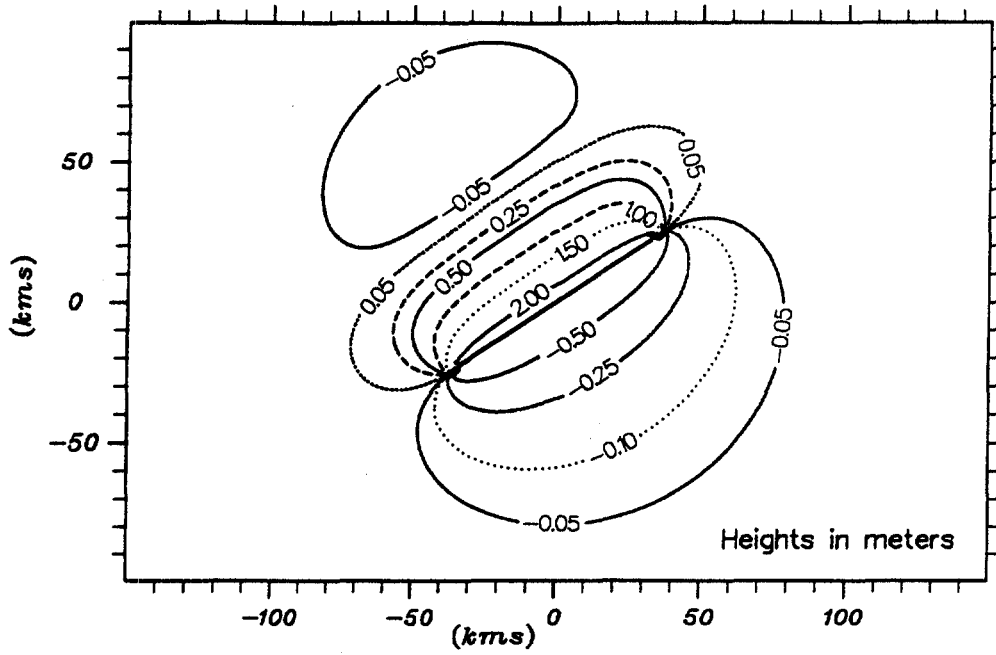


Figure 3. Computed vertical ground displacement for a N55°E fault orientation

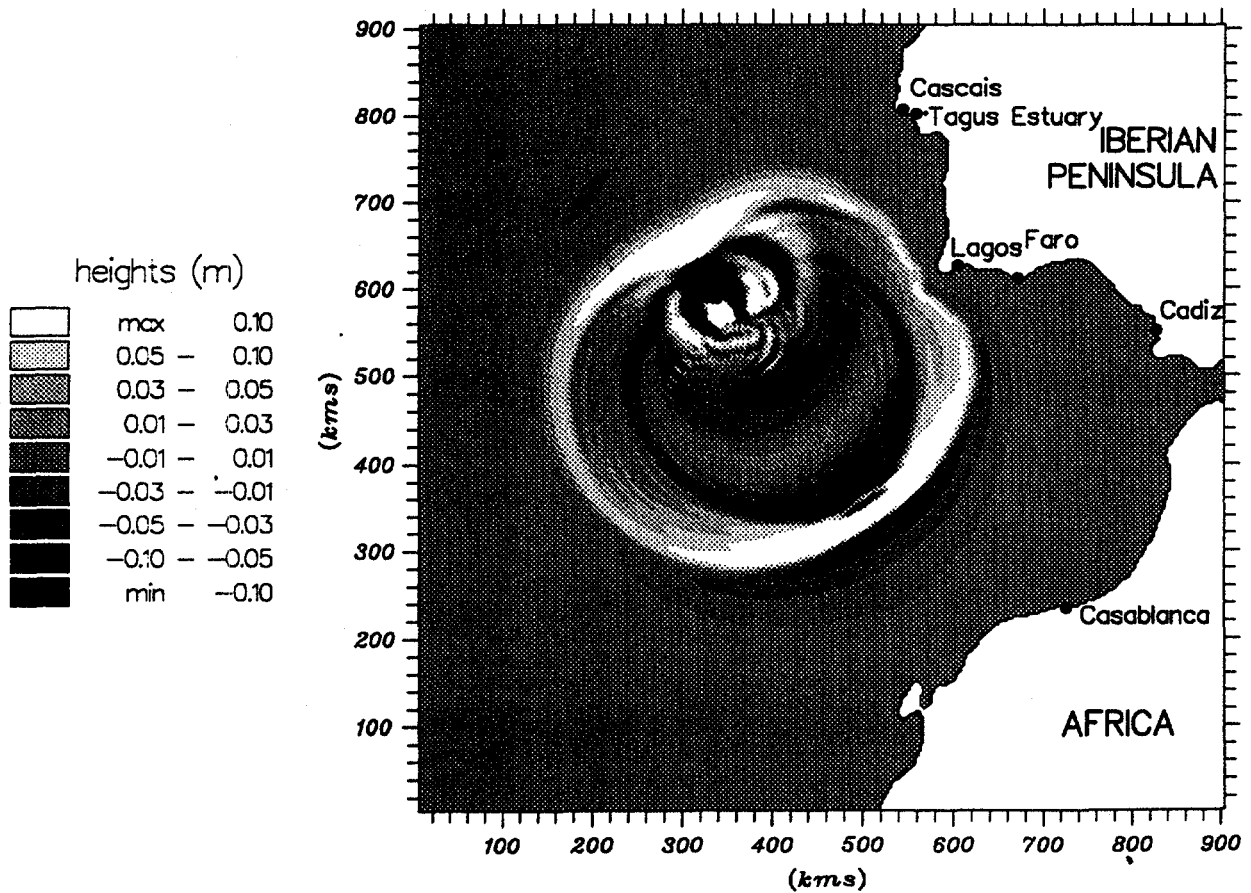


Figure 4. Computed water surface at t=1000s, using a shallow water model

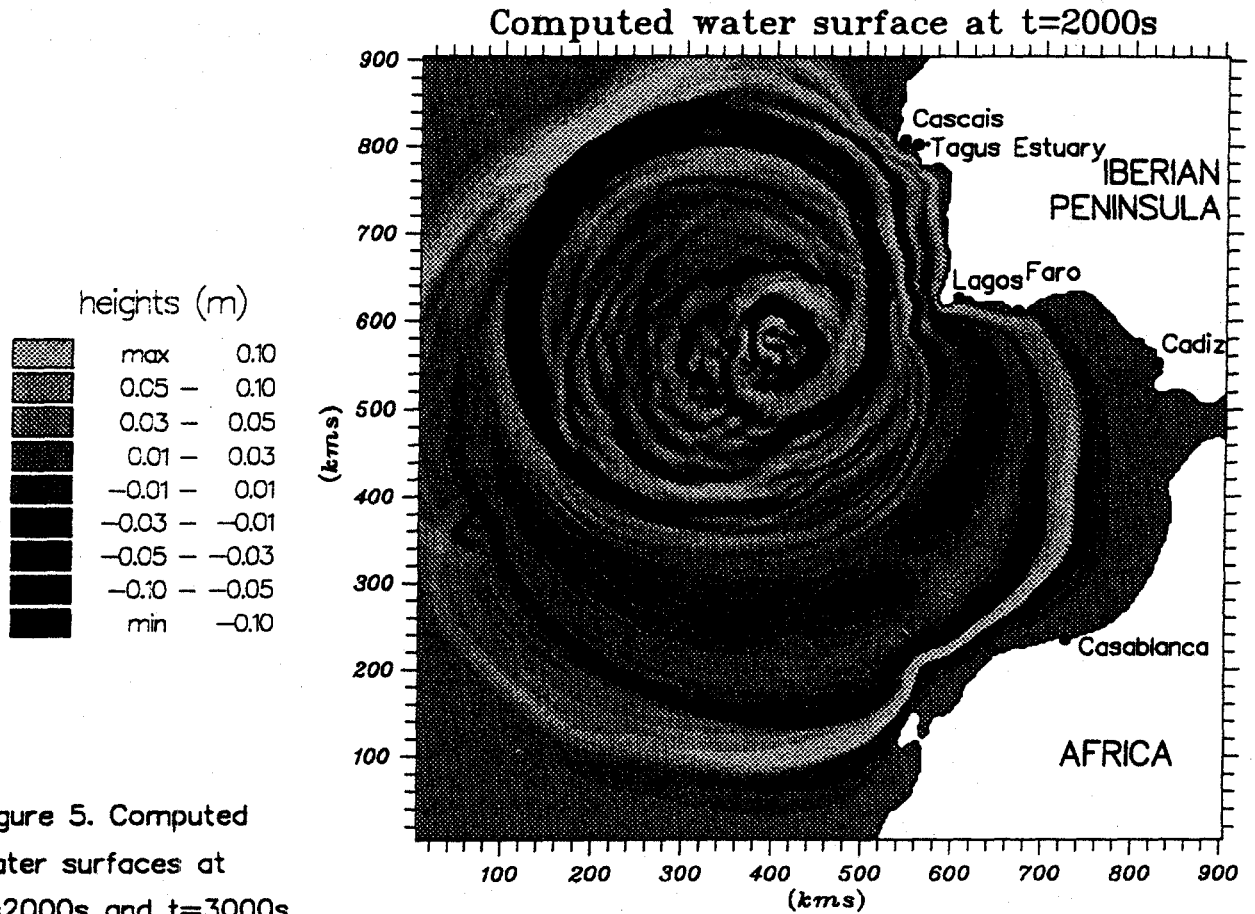
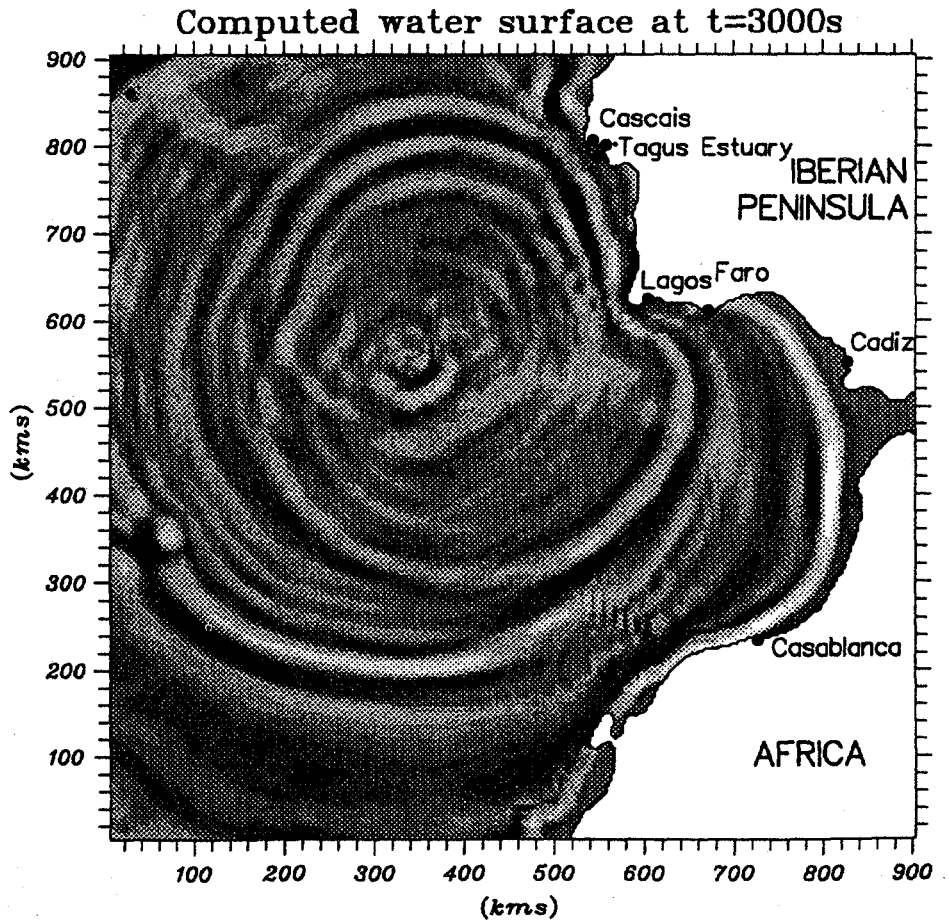


Figure 5. Computed water surfaces at t=2000s and t=3000s, using a shallow water model



Computed water surface at t=5000s

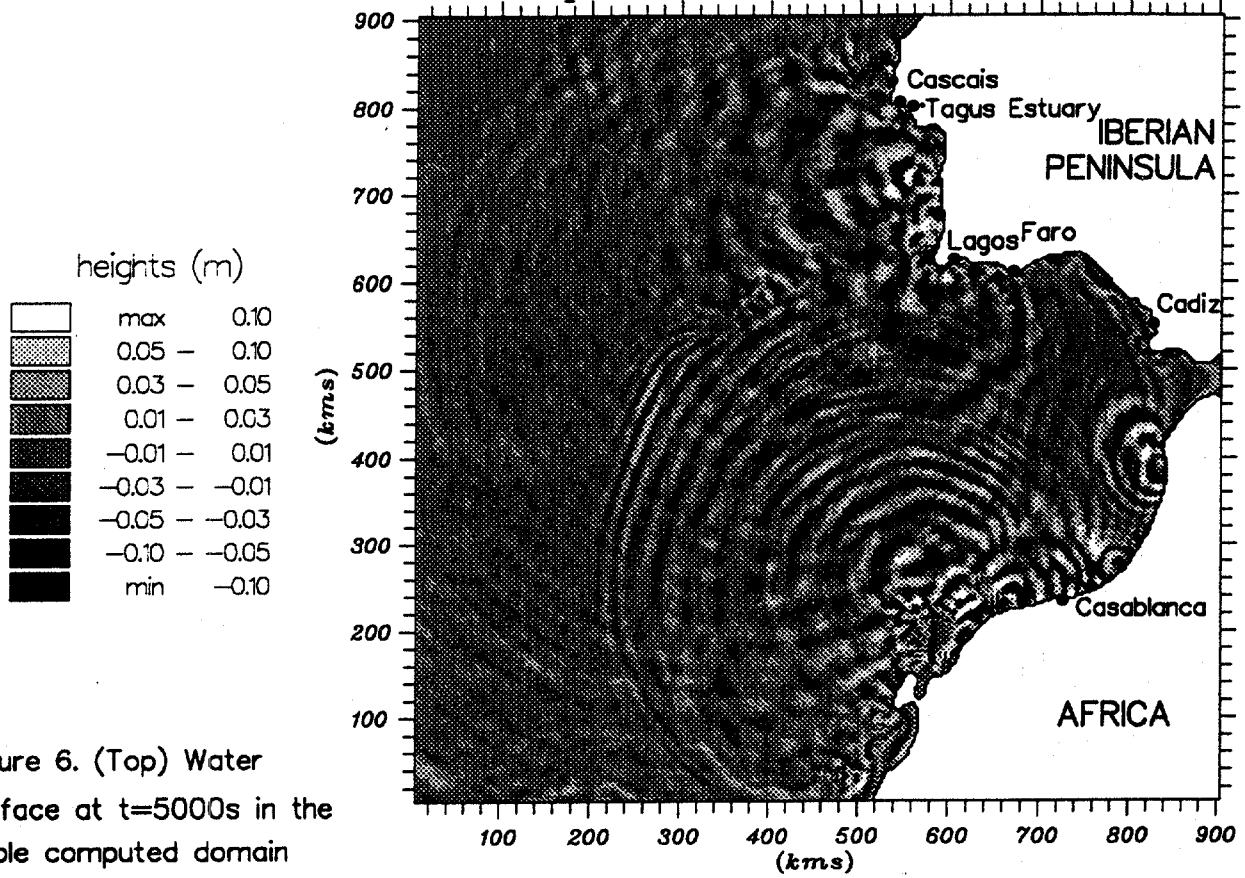
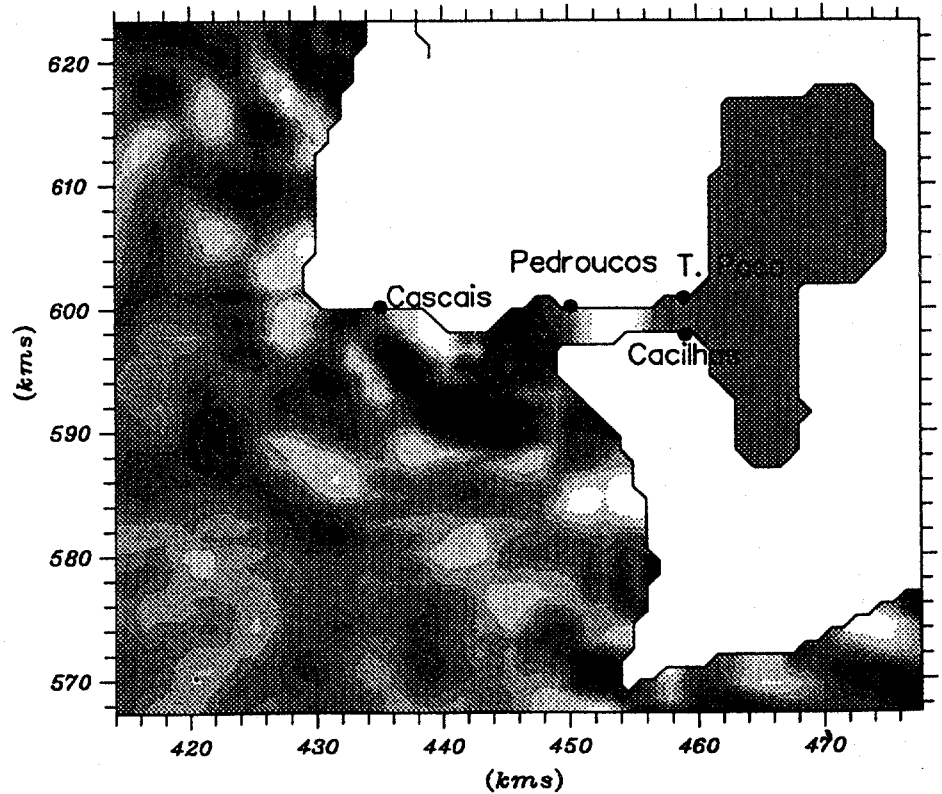


Figure 6. (Top) Water surface at t=5000s in the whole computed domain

(Bottom) Water surface at t=4000s in the Tagus Estuary. Location of the tide gauges

Computed water waves at t=4000s



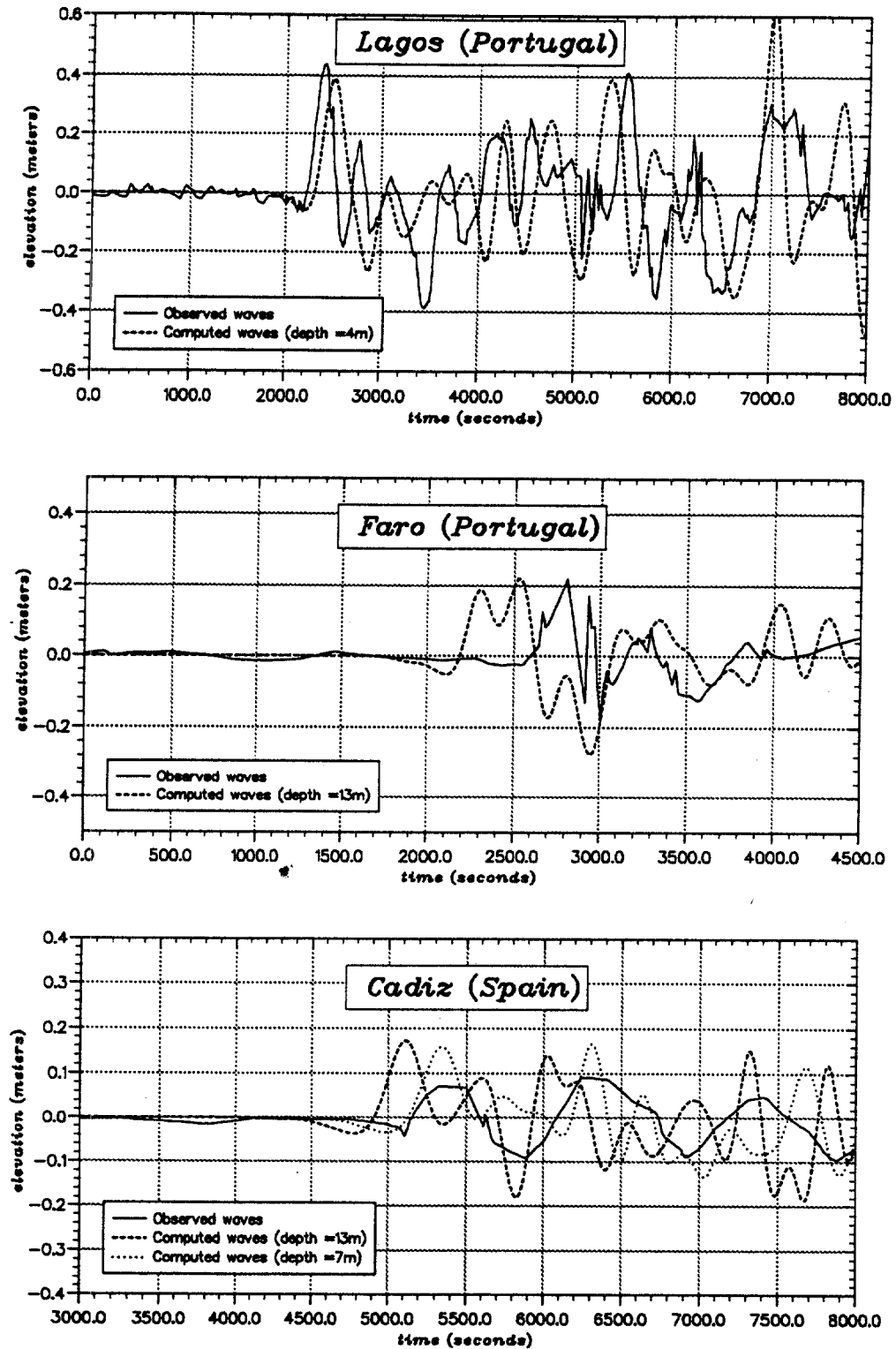


Figure 7. Comparison between observed and computed waves at Lagos, Faro and Cadiz

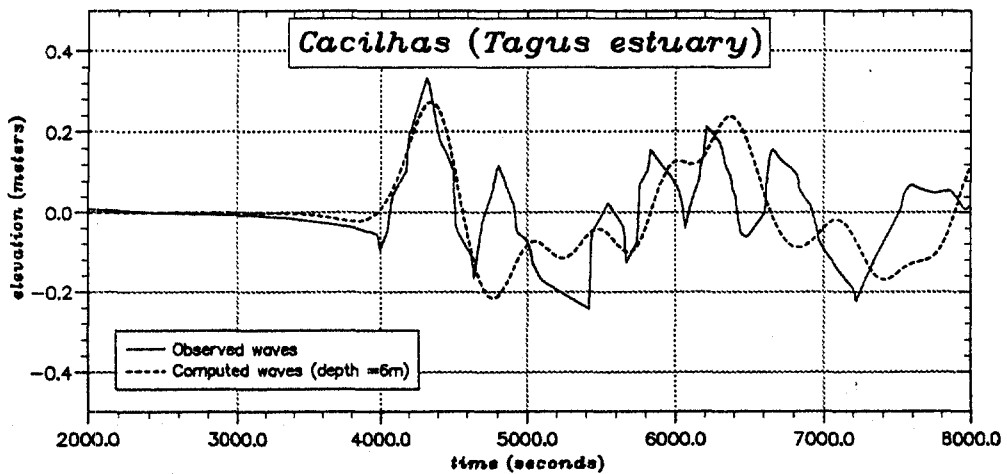
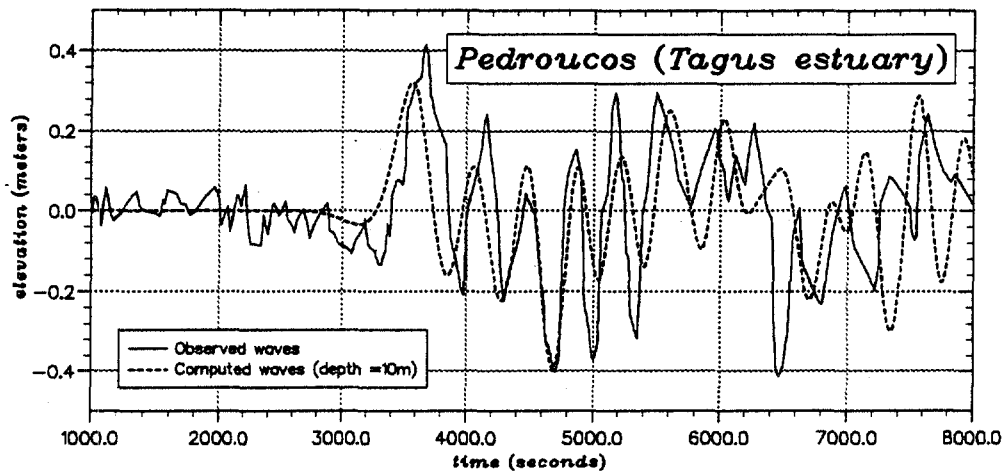
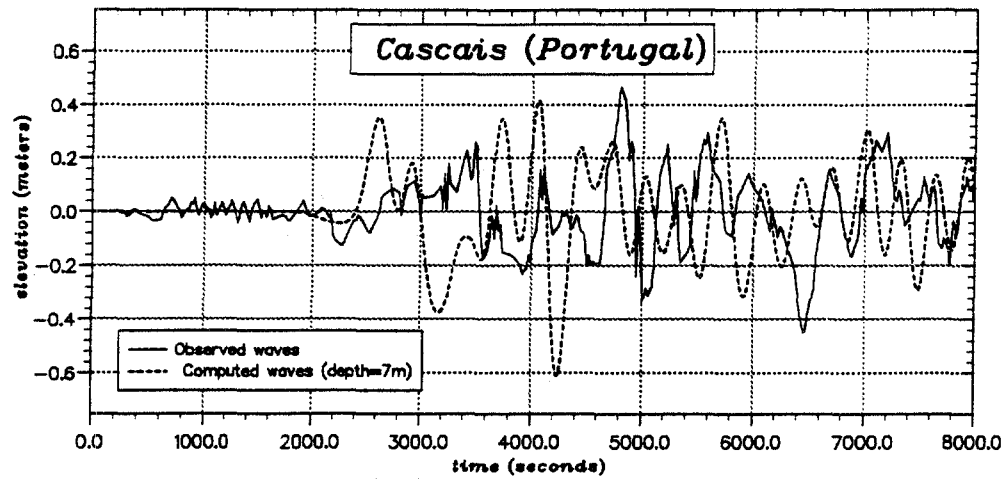


Figure 8. Comparison between observed and computed waves at Cascais, Pedroucos and Cacilhas

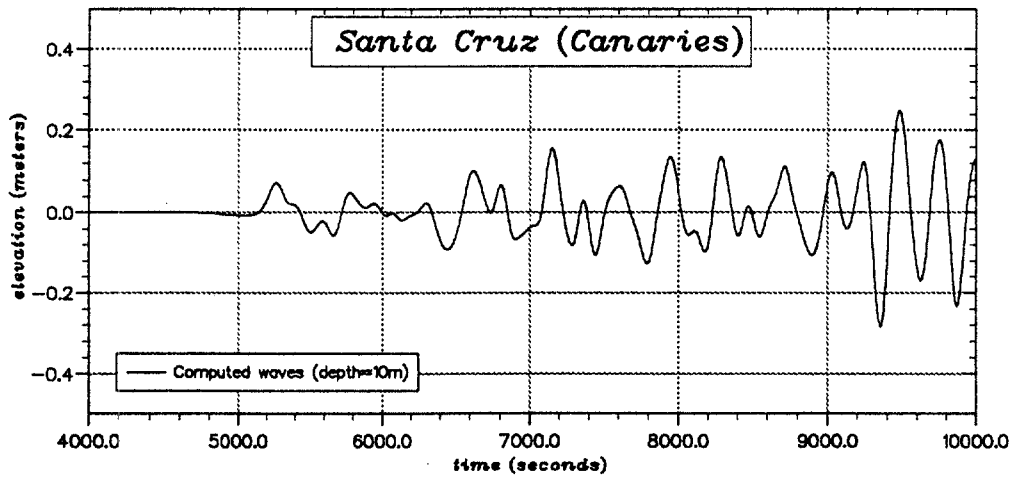
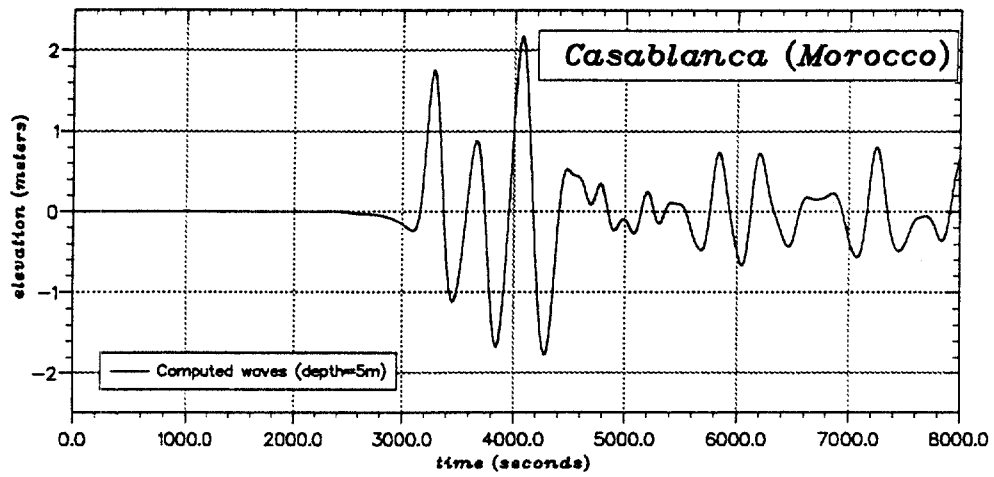
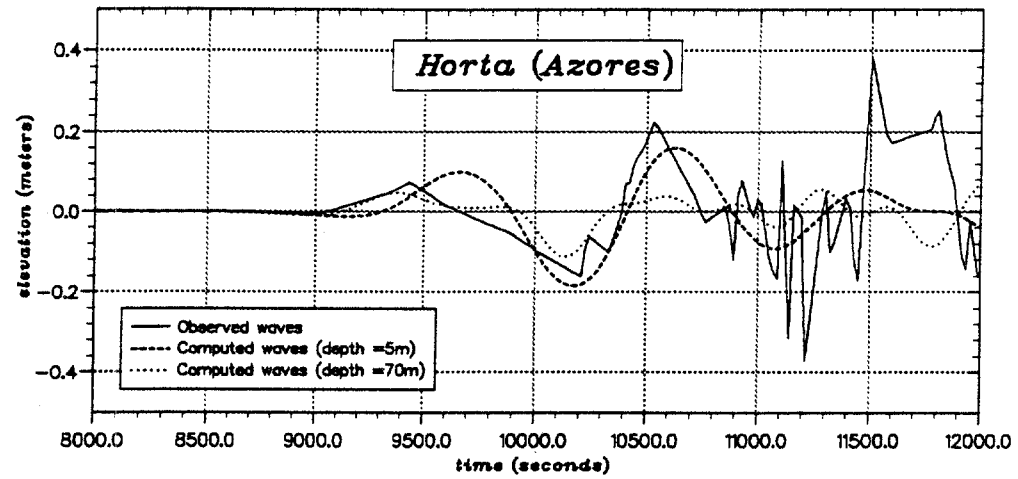


Figure 9. Comparison between observed and computed waves at Horta
 Computed waves at Casablanca and Santa Cruz de la Palma

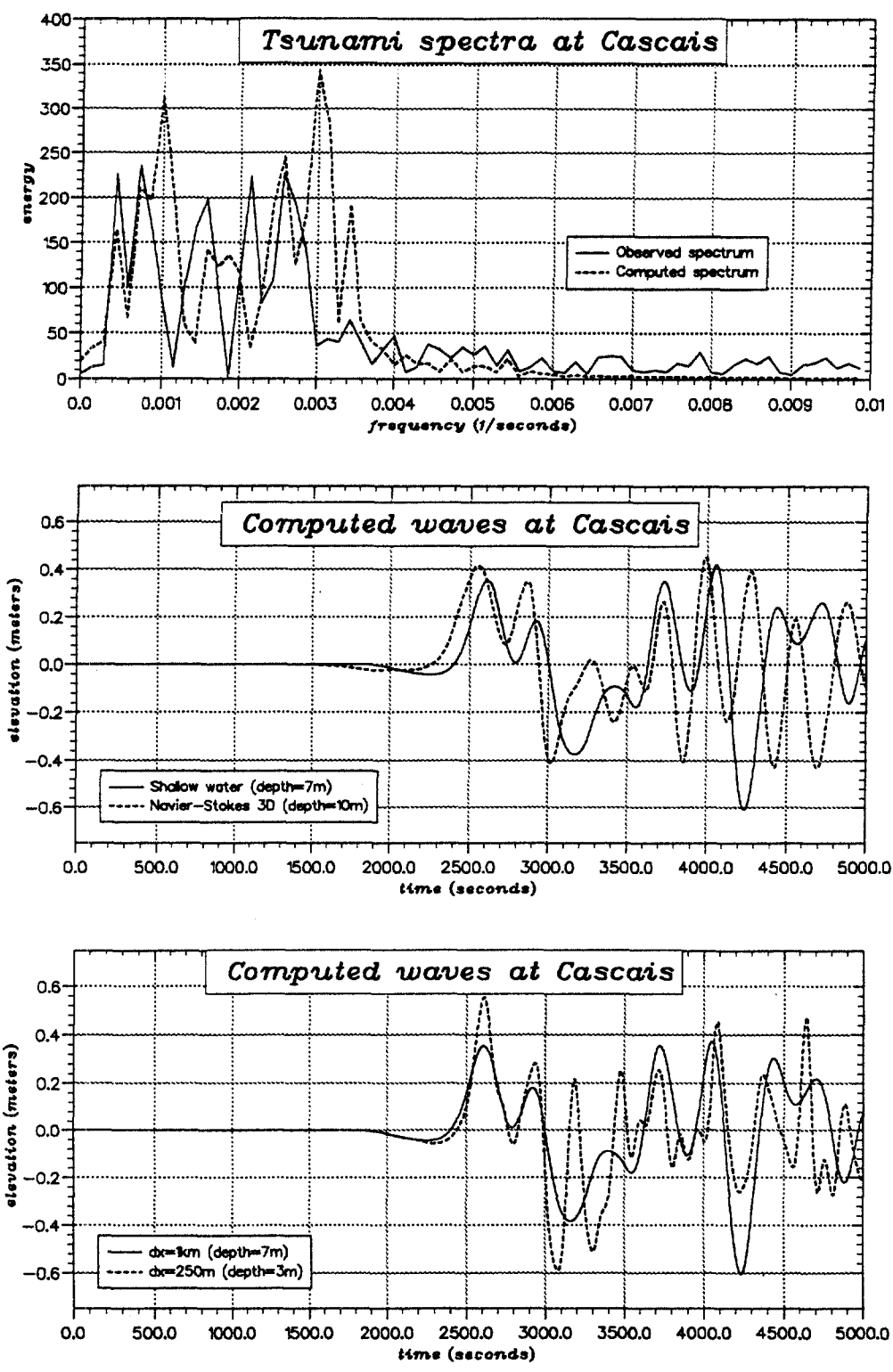


Figure 10. (Top) Comparison between observed and computed spectra at Cascais
(Middle) Numerical results obtained by the 3D Navier–Stokes model
(Bottom) Shallow water simulations with different cell sizes

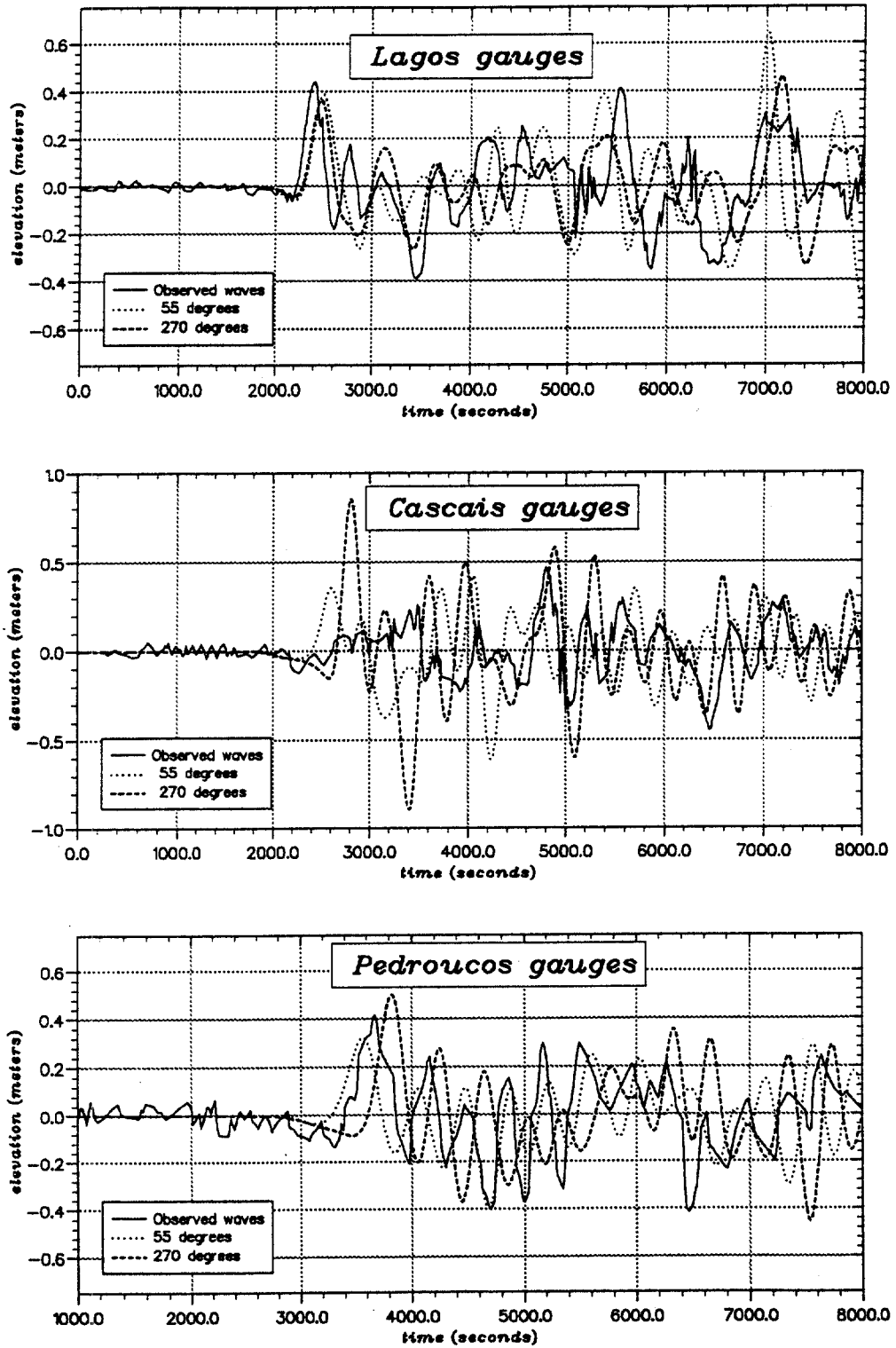


Figure 11. Comparison between observed and computed waves for two different striking faults

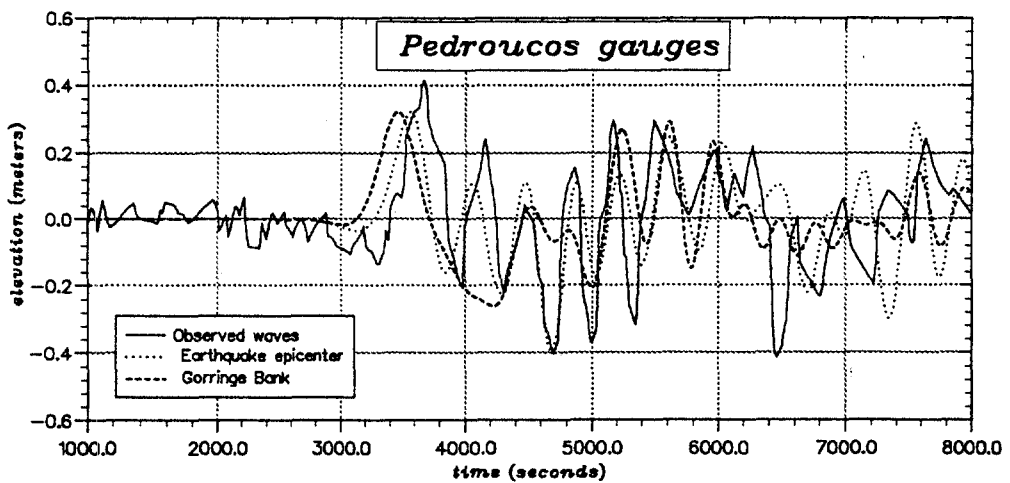
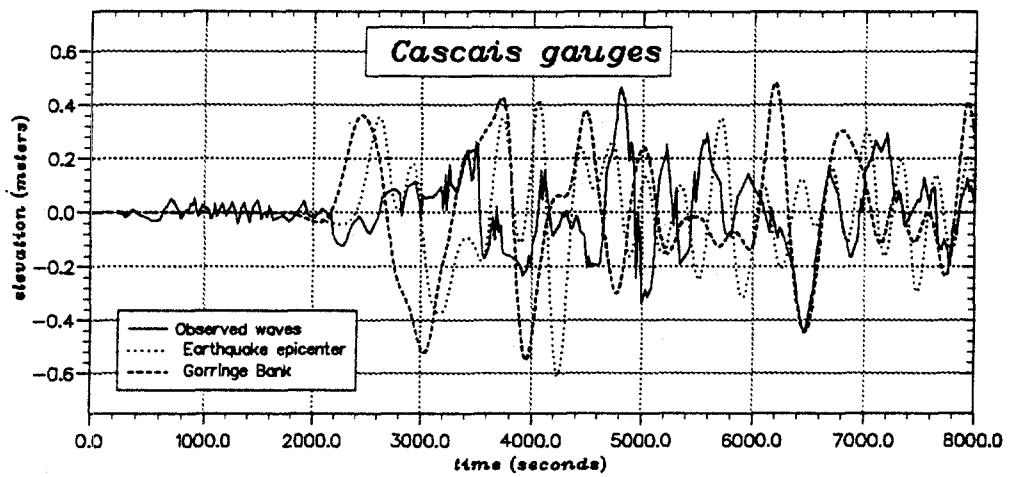
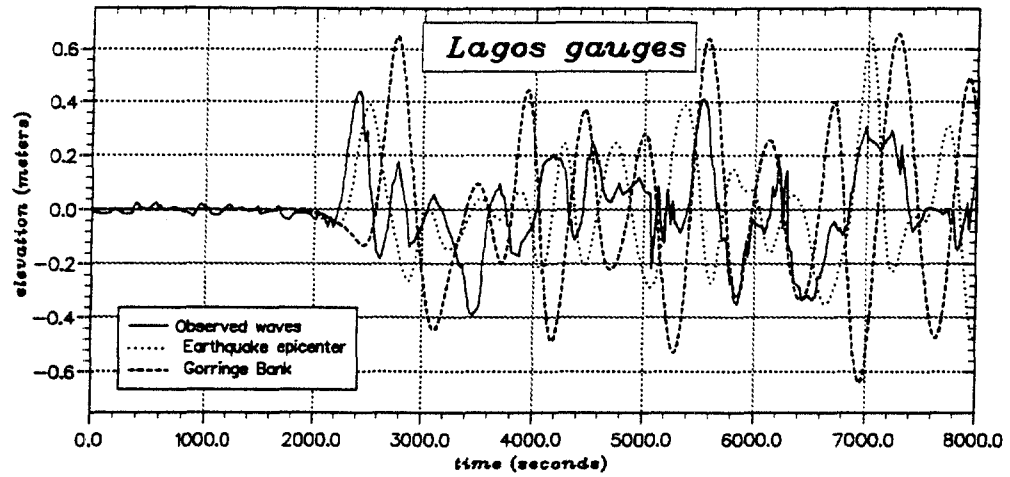
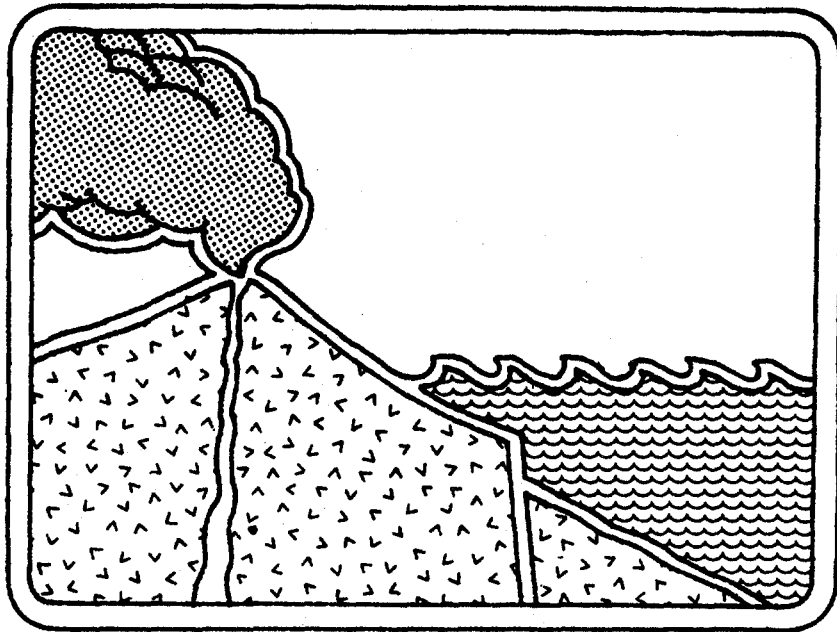


Figure 12. Comparison between observed and computed waves for two different source locations



**ON THE INFLUENCE OF THE SIGN OF THE
LEADING TSUNAMI WAVE ON THE HEIGHT
OF RUN-UP ON THE COAST**

S. L. Soloviev

Institute of Oceanology

Russian Academy of Science, Moscow, Russia

R. Kh. Mazova

N. Novgorod State Technical University

Nizhny Novgorod, Russia

ABSTRACT

None of the known tsunamis in the Pacific Ocean began in all regions of the coast with the ebb but the majority of tsunamis came in as positive waves. If positive and ebbs were observed simultaneously, positive waves predominated and negative ones were observed along limited places of coasts close to tsunami sources. This reflects the tectonic compression of the Pacific basin. If the positive wave comes first to the coast, the maximum run-up may occur for one of the waves following the leading wave. Such a possibility is confirmed by an analytical treatment. If a negative leading wave of the same height arrives, the run-up may be highest for the first wave.

INTRODUCTION

Tsunami waves may achieve a considerable height resulting from a tremendous natural calamity on the Pacific coast of Kamchatka and the Kuril Islands (1), other coasts of the Pacific Ocean (2, 3, 4), in many regions of the Mediterranean Sea (5), and in a number of regions of the Atlantic and Indian Oceans (6). The opinion that the tsunami wave train approaches the coast as a crest (a tidal wave of the positive phase) is rather popular, but it is erroneous in principle. However, the analysis of natural data shows that tsunamis often begin on the coast as an ebb. But there are neither statistical data, nor the subsequent analysis of this evidence yet. The sign of the leading tsunami wave may change both due to its propagation along the peculiarities of the underwater relief and due to its interaction with the coast (trapped waves). However, proceeding from modern concepts of tsunami formation, one should consider that this sign reflects the direction of the vertical shift of the sea bottom in the tsunami source: a rapid seismotectonic rise of some regions of the bottom should result in the emergence of tsunami approaching the coast by the crest, while the descent of some regions should result in tsunami approaching by the cavity (7-13). In this connection studying the directivity (signs) of the first tsunami wave is of interest for better understanding of both the mechanism of the source of a separate tsunamigenous earthquake and the modern tectonic processes in the Pacific Ocean on the whole.

Looking through the catalogues of tsunamis in the Pacific Ocean (2, 3, 4) shows that no tsunami was registered that would begin in all points of the coast as an ebb. This allows us to conclude that the bottom of the Pacific Ocean upon the whole is in the state of compression (this is confirmed by the existence of shear zones along the ocean periphery - seismofocal Vadati-Zavaritsky-Beniof layers). None of the tsunamis occur due to the depressive fall of the sea bottom.

If we ascribe the sign "plus" to the run-up of the wave with the positive phase and the sign "minus" to the rundown wave, all the tsunamis considered may be divided into two types: 1 - tsunamis consisting completely of pluses, 2 - tsunamis consisting mainly of pluses with negligible number of minuses, concentrated as a rule on the coast which is the nearest to the tsunami source. The latter may be illustrated by the fact that such well-studied tsunamis occurred in Alaska (March 27-28, 1964), Niigata (June 16, 1964), the Sea of Japan (May 26, 1983) were actually caused by rapid rises of vast bottom regions, surrounded from the coast side by a narrow (in width) and insignificant descent of the bottom (12, 13 14) according to the classification made above, these tsunamis refer to the second type. The present paper deals mainly with the problem of the necessity to take into account the sign of the leading tsunami wave, when estimating the expected tsunami run-up.

STATISTICAL ANALYSIS

The analytical estimate of the run-up of the tsunami wave train on the coast (15, 16, 25) may show that:

1. Not only the first wave (positive) in the train, but the wave following may have the maximum height.
2. The maximum run-up of the train with the first negative phase may be greater than that of the train with the leading positive wave (for one and the same initial conditions).

3. The wave that follows the rundown may have a steep profile and a high velocity (as compared to the first wave).

We shall verify these conclusions by analysing the natural data on the tsunami waves run-up on the coast. We use the actual data on the tsunami from the catalogues (2, 3, 4), the Shchetnikov set of mareograms (18, 19) and other works (20). The analysis was performed for the four main types of the beginning of the tsunami climbing process on the coast: I - water rise on the coast in the form of a quiet inundation, II - run-up of the visible water step (bore) of the arbitrary form, III - by unexpected quiet ebb of the coastal zone, being as a rule lower than the usual minimum level of ebbs, IV - the ebb of the visible wave (negative bore). The analytical estimates (15, 16) allow us to make the conclusion that at one and the same geometry of the problem and the initial wave energy, the run-up of the waves of III and IV types may result in significantly greater destruction in the coastal zone than that of the waves of I and II types. Unfortunately, we have at our disposal neither complete visual information for strong tsunamis that occurred many years ago (the phase of the first wave arrival, the height of the second and the third wave), nor mareograms for the majority of tsunamis. Thus, we cannot estimate them quantitatively and compare them with our analytical results (15, 16, 17).

In the connection for quantitative estimates we have used the papers (4, 18, 19), where mareographic data on the Pacific tsunamis that occurred from 1952 to 1985 were given. The analysis is based on the tables with the data on the first and maximum waves as well as mareograms. We should mention here that it follows from (21) that the values of the visual run-up differ statistically from the mareographic water rise by the factor of square root of 2. Therefore, the use of tables and mareograms for estimating the actual run-up has such an accuracy. Besides, it follows from natural observations that the maximum waves as a rule are the first to third waves in the train, thus to estimate the effect of the first phase on the value of the run-up we used the maximum wave data corrected with the corresponding mareographs. For the analysis of 84 cases when tsunamis began with the rundown and 335 cases when tsunamis began with the run-up were chosen. A number of functional dependences were obtained on the basis of these data. The dependences for the run-up of the wave train were plotted. Figure 1 gives the height of the maximum water rise H_{max} as the function of the amplitude of the first wave H which is positive for the first type of waves (curve 1) and negative, but taken in absolute value, for the third type (curve 2). We have obtained the following:

$$H_{max}^+ = 0.6H_1 + 6.0 \quad (1)$$

$$H_{min}^- = 1.2H_1 + 5.9 \quad (2)$$

It is seen that the curve for the tsunamis beginning with the rundown is more steep than for the waves beginning with the run-up. This may testify that the amplitude of the maximum wave that follows the rundown is greater as a rule than that of the leading wave of the run-up in the considered case (type II). Thus for example at $H = 100cm$, H_{max}^- is twice as large as H_{max}^+ . The curve for Yuzhno-Kuril'sk was additionally plotted for the

cases when tsunamis began with rundown (curve 3). For these cases: $H_{max} = 0.8H_1 + 3.9$. The data are taken from Table No. 12 of (19) using 23 tsunamis of the 63 tsunamis observed in this region during 1957-1982 that began with run-down. One may see that this dependence is also more strong than (1).

On the basis of 419 cases of tsunami histograms of height distribution of waves of different types approaching the coast by the crest (1) and by the cavity (2) are plotted in figure 2. It is readily seen from the figure that in both cases the character of the distribution, as it should be expected, is the same. Thus when processing sea wave data (22, 23, 24), these histograms are fairly well equalized by the right branch of the normal distributions:

$$N_1 = 1.2 * 10 * \exp(-(H/H_1 + 0.3)^2/2) \quad (3)$$

$$N_2 = 1.3 * 10 * \exp(-(H/H_2 + 0.5)^2/2) \quad (4)$$

The curve describing the tsunami repeatability when the wave train approaches the coast by the crest (2), lies higher than the curve for the tsunami beginning with the trough (1). This may be the evidence that the tsunami of the types I and II predominate over those of types III and IV. The tsunami repeatability may be also expressed by the power relation (which is more convenient for seismologists) that in the double logarithmic scale has the format:

$$\lg(N/N_\sigma) = -1.5\lg(H) - 0.062 \quad (5)$$

where N_σ is the total number of the considered cases.

These statistical results were obtained by analysing weak events with the amplitude of the approaching wave from 4 to 150 cm. Therefore, the problem on the possibility of the use of these results for the comparative analysis in a more general case may be of interest. For this we solve the problem of the verification of the homogeneity of the statistic material. For the analysis we may take two independent samplings X_1 and X_2 for the first one being the sampling of the tsunamis of large amplitude considered in paper (20) and the second one being the sampling of the tsunamis beginning with water rundown from the coast. (We may consider also the sampling for weak waves of the tsunamis of the I and III types). It is necessary to ascertain whether these are the samplings from one and the same distribution or the distribution law is different. In the first case all the conclusions made for one of the distributions are valid also for the other. The repeatability law plotted for the sampling X_1 (the dotted line in Figure 2) has the form (20), while for the sampling X_2 we have correspondingly the formula (3). To verify the hypothesis of the homogeneity, we may use the integral distribution functions, formally obtained from the distribution of (3) and (20) correspondingly. We have shown that our assumptions that X_1 and X_2 are the samplings of one and the same distribution. Thus the results obtained by analysing the run-up of small-amplitude waves on the coast are valid also for more strong tsunamis.

Conclusions

1. When calculating tsunami risk it is necessary to take into account the fact that a wave train may approach the coast with various initial phases, since the maximum run-up is essentially determined by the sign of the leading wave. In this case the leading wave is not obligatorily the maximum one.

2. When tsunami waves climb the coast such waves prevail that approach the coast by the crest. This indicates that the bottom in the Pacific Ocean is currently compressed.

3. When calculating tsunami risk it is necessary, if possible, to take into account the sign of the vertical shift of the ocean bottom in the tsunami source which may be often determined by seismograms.

4. To study the mechanism of the excitation of a tsunami, one should thoroughly study tsunami emergence on the coast, taking into account the phase of the first wave.

LITERATURE

1. S. L. Soloviev, "The Tsunami Problem and Its Significance for Kamchatka and Kuril Islands," *The Tsunami Problem*, Nauka Press, Moscow pp 7-50, (1968) in Russian.
2. S. L. Soloviev, Ch. N. Go, "The Catalogue of Tsunamis of the West Coast of the Pacific Ocean," Nauka Press, Moscow (1974) in Russian.
3. S. L. Soloviev, Ch. N. Go, "The Catalogue of Tsunamis of the East Coast of the Pacific Ocean," Nauka Press, Moscow (1975) in Russian.
4. S. L. Soloviev, Ch. N. Go, and Kh. S. Kim, "The Catalogue of Tsunamis of the Coast of the Pacific Ocean 1969-1982," MGK Press, Moscow (1985) in Russian.
5. S. L. Soloviev, "Mediterranean Sea Tsunamis and their Comparison with Pacific Ocean Tsunamis," *Fizika Zemli*, No. 11, pp 3-17, (1989) in Russian.
6. I. D. Ponyavin, "The Tsunami Waves," *Gidromet Press, Leningrad* (1989). in Russian.
7. I. Adia, "Numerical Experiment for the Tsunami Propagation - The 1964 Niigata Tsunami and the 1968 Tokachioki Tsunami," *Bulletin Earthquake Rec. Institute, University of Tokyo*, Vol 47, pp 673-700 (1969).
8. I. Aida, "Reliability of a Tsunami Source Model Derived from Fault Parameters," *Journal Physics of Earth*, Vol 26, pp 57-73 (1978).
9. T. Hatori, "On the Tsunami which Accompanied the Earthquake Off the North-West of Oga on May 7, 1964," *Bulletin Earthquake Rec. Institute, University of Tokyo*, Vol 43, pp 149-159 (1965).
10. T. Hatori, "Vertical Crucial Deformation and Tsunami Energy," *Bulletin Earthquake Rec. Institute, University of Tokyo*, Vol 48, pp 171-188 (1970).
11. T. Hatori, "Tsunami off the Nemuro Peninsular in June 1973 and Tsunami Generation in East Hokkaido," *Royal Society of New Zealand bulletin* 15, pp 61-70 (1976).
12. T. Hatori, "Tsunami Magnitude and Source Area of the Nihonkai-Chubu(the Japan Sea) earthquake in 1983," *Bulletin Earthquake Rec. Institute, University of Tokyo*, Vol 58, pp 723-734 (1983).
13. L. Sh. Hwang, D. Divoky, "Tsunami Generation," *Journal Geophysical Research*, Vol 75, No 33 (1970).
14. S. L. Soloviev, A. N. Militeev, "Emergence of Niigata Tsunami 1964 on USSR Coast and Some Data on Wave Source," *The Tsunami Problem*, Nauka Press, Moscow pp

- 213-231 (1968) in Russian.
15. T. S. Golubtsova, R. Kh. Mazova, "Run-up on a Beach of Waves with Sign-Alternating Form," *Oscillations and Waves in Solid State Mechanics*, Gorky Polytech. Institute Press, Gorky, pp 30-42 (1989) in Russian.
 16. R. Kh. Mazova, N. N. Osipenko, "The Influence of form of Long Wave Approaching the Beach on Run-up Characteristics," *Oscillations and Waves in Liquids*, Gorky, pp 71-82 (1988) in Russian.
 17. R. Kh. Mazova, E. N. Pelinovsky, "The Increasing of Tsunami Runup Heading Wave," *Symp. Digest of IV Int. Symp on Geophys. Hazards* (1991).
 18. N. A. Shchentnikov, "Mareogram Atlas, IMGIG DVNC USSR," Academy Science Press, Vladivostok (1990).
 19. N. A. Shchentnikov, "Tsunamis on the Coast of Sakhalin and Kuril Islands from Mareographic Data 1952-1968, IMGIG DVNC USSR." Academy Science Press, Vladivostok (1990) in Russian.
 20. R. Kh. Mazova, E. N. Pelinovsky, S. L. Soloviev, "Statistical Data on the Character of Runup of Tsunami Waves," Gorky, Preprint No. 58, IAP of USSR Academy of Science Press, Gorky (1982) in Russian.
 21. S. L. Soloviev, "Tsunamis," *Assessment and Mitigation of Natural Hazards*, UNESCO, Paris, pp 118-134 (1979).
 22. S. L. Soloviev, "Repeatability of Earthquakes and Tsunamis in Pacific Ocean," *Tsunami Waves, Sakhalin Research Institute of USSR, Academy of Science Press, Yuzhno-Sakhalinsk*, No. 29, pp 7-47 (1972).
 23. G. E. Kononkova, K. V. Pokazeev, "Sea Wave Dynamics," Moscow University Press, Moscow (1985) in Russian.
 24. *Theoretical Basis and Counting Methods for Wind Waving*, Gidromet Press, Leningrad (1988) in Russian.
 25. G. I. Ivchenko, Yu. I. Medvedev, *Mathematical Statistics*, High School Press, Moscow (1984) in Russian.

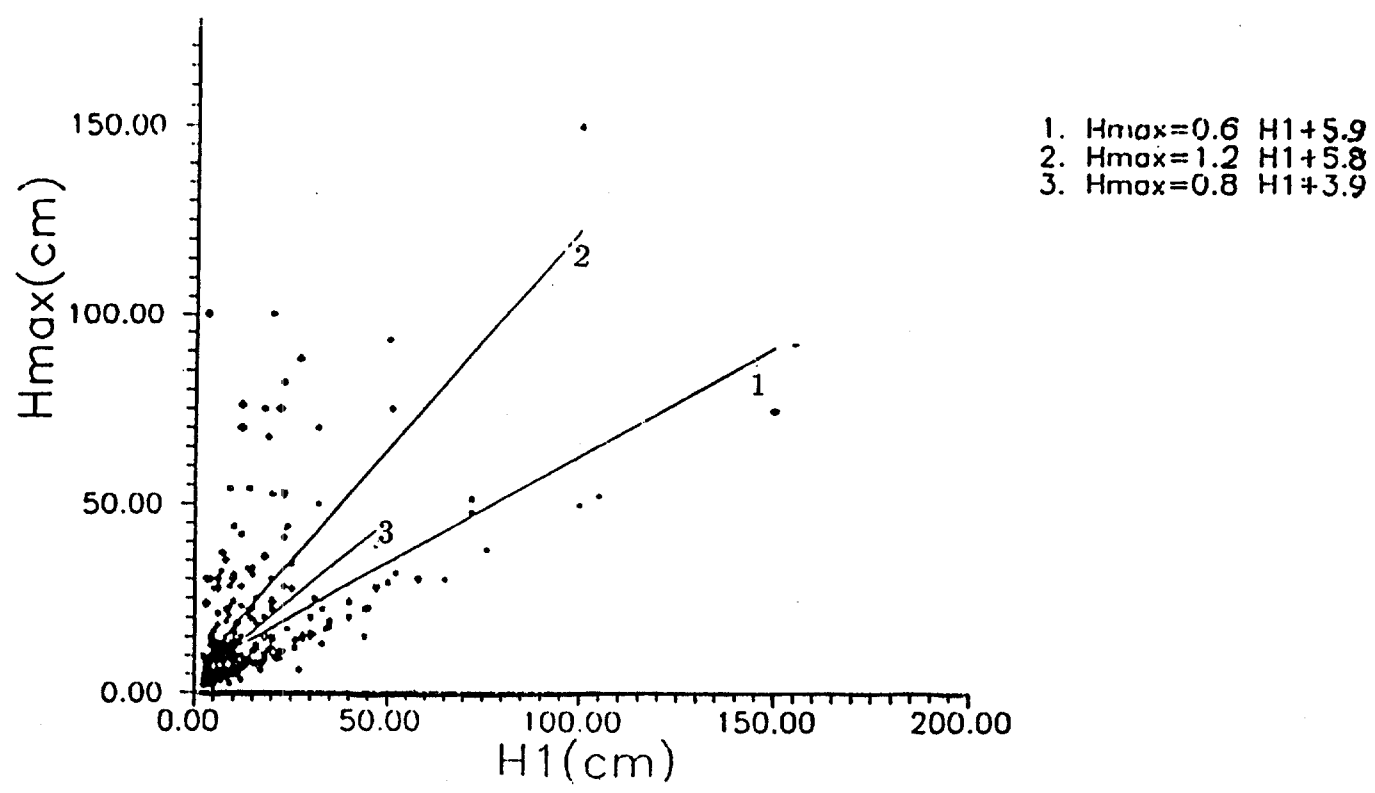


Figure 1. The dependence of the maximum water rise on the coast (H_{max}) on the amplitude of the first wave (H_1). 1 - the run-up wave. 2 - tsunami beginning with the ebb-tide. 3 - tsunami beginning with ebb-tide for Yuzhno-Kuril'sk.

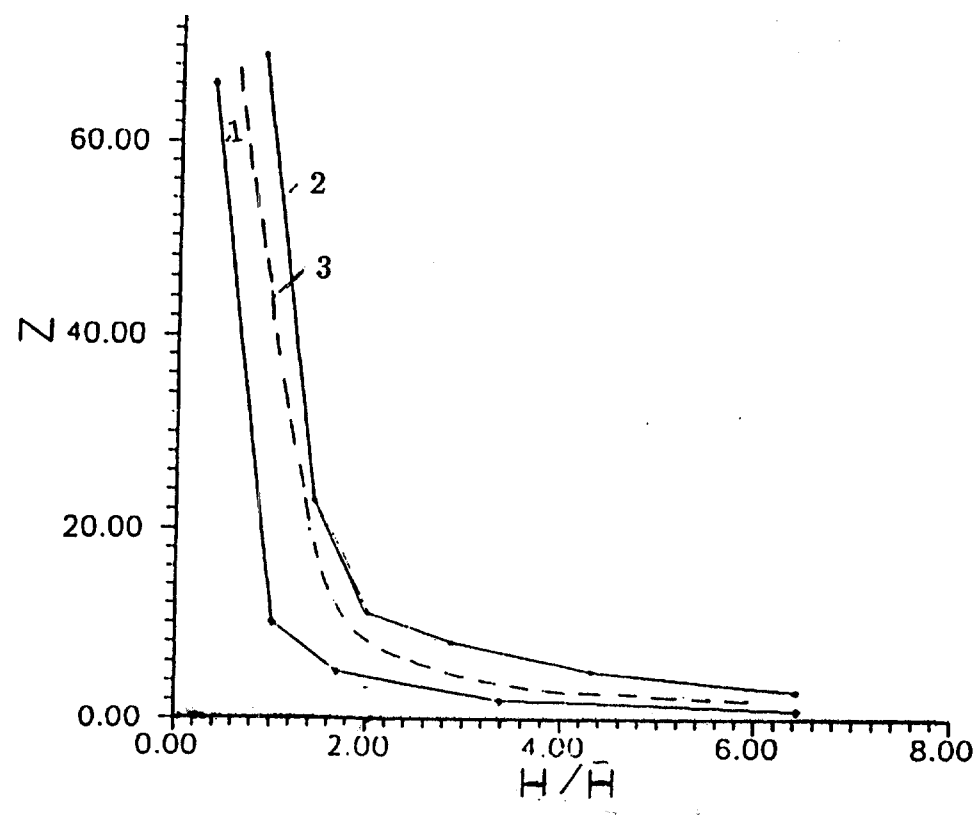
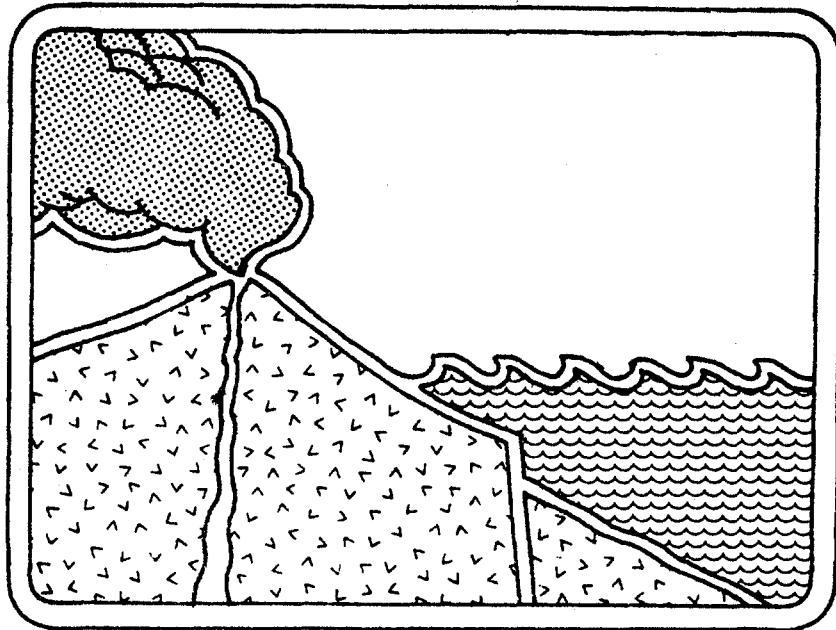


Figure 2. Histograms of the height distribution of tsunamis of various types (see text).



MODELING THE 105 Ka LANAI TSUNAMI

Carl Johnson

Department of Geology

University of Hawaii, Hilo, HI., U.S.A.

Charles L. Mader

Senior Fellow, JTRE - JIMAR Tsunami Research Effort

University of Hawaii, Honolulu, HI., U.S.A.

ABSTRACT

Approximately 105,000 (105 Ka) years ago, tsunami waves are believed to have occurred that swept up to current elevations of about 325 meters on the island of Lanai and to lower levels on other Hawaiian islands. The lower sea level of 105 Ka would require a wave of over 400 meters. Recent sonar surveys of the Hawaiian Ridge show slumps and debris avalanches which are more than 200 kilometers long and 5000 cubic kilometers in volume. This study was undertaken to determine if any of these underwater landslides could be the source of the 105 Ka Lanai tsunami.

The modeling was performed using the *SWAN* code which solves the nonlinear long wave equations. The tsunami generation and propagation was modeled using a 1.0 and a 0.5 minute grid of the topography of the Hawaiian Islands. Of the various known debris avalanches, the age and geographic constraints suggest that the movement of the Alike 2 debris avalanche off the Kona coast of the island of Hawaii was the most likely tsunami generating source. To obtain a Lanai runup of over 300 meters, a landslide of 160 cubic kilometers and uplift of 1000 meters was required.

THE LANAI TSUNAMI

As described in references 2 thru 7, approximately 105,000 years (105 Ka) ago based on uranium-series dating, a series of coral-bearing gravels were deposited on the Hawaiian islands, probably by a tsunami wave, that reach 326 meters above current sea level (375 to 425 meters relative to sea level at time of the waves) on the island of Lanai and 60 to 80 meters on the islands of Oahu, Molokai, Maui and Hawaii.

Possible origins of such large waves are (1) submarine volcanic explosion, (2) impact of a meteorite in the ocean near Hawaii, and (3) local submarine landslides. In reference 2, Moore and Moore proposed that the tsunami wave was formed by the failure and downward movement of a landslide on the slope 50 kilometers southwest of Lanai. Sea-floor imaging of the slope southwest of Lanai with the Gloria sidescan sonar system has identified a submarine landslide called the Lanai slide. The slide is about 40 km wide at the top beginning in water less than 2000 meter deep. The area of its toe extends to a depth of 4,500 meters. To examine the nature of the wave from a massive Lanai slide, we modeled the slide as a 10x50x2 kilometer drop down the slope and a 20x50x1 kilometer uplift along the ocean floor. Such a slide covers all the area of the Lanai slide and is probably at the upper limit of disturbance possible from such a slide. The calculated wave characteristics near the shore of the Hawaiian islands are given in Table 1. The highest amplitude near Lanai was only 60 meters which indicated that the Lanai slide is an unlikely candidate for the source of the 325 meter high Lanai tsunami.

In reference 6, Moore, Normark and Gutmacher state that age and geographic constraints suggest that the movement of the Alika 2 debris avalanche generated the waves that deposited the dated gravels on Lanai. Three well-defined debris avalanches, the South Kona, Alika 1, and Alika 2 landslides drape the submarine west flank of the currently active Mauna Loa volcano on the island of Hawaii. The upper reaches of the Alika debris avalanches extend from the shoreline down to 2 kilometers. The middle course of the avalanche has a 40 kilometer long flat-floored channel that is 10 kilometers wide. The broad lobe at the lower part of the Alika 2 debris avalanche is 34 kilometers in diameter. The combined volume of the Alika landslides is 200 to 800 cubic kilometers.

In reference 7, Johnson and King described the Alika landslide off the coast of Kona as a drop of 20x20x1.5 kilometers down the island slope and an uplift of 28x28x0.75 kilometers on the ocean floor maintaining the volume of 600 cubic kilometers. This landslide was modeled using a one minute grid of the Hawaiian island chain topography. As shown in Table 2 the Johnson and King Alika landslide model resulted in a wave with a height of about 100 meters in shallow water near the island of Lanai which would at most double in amplitude as it shoaled. The landslide would not cause the observed 400 meter high 105 Ka Lanai tsunami. To determine the size of landslide required, we increased both the landslide size and the amplitude. As shown in Table 2, we had to increase the landslide volume to 1600 cubic kilometers to double the wave amplitude near the coast of Lanai. To examine the shoaling of this wave on the island of Lanai, the cell size was decreased to 0.5 minute.

MODELING THE LANAI TSUNAMI SHOALING

The generation and propagation of large historical Hawaiian landslide tsunamis was modeled using a 1.0 and a 0.5 minute topographical grid of the Hawaiian Islands topography. The modeling was performed using the *SWAN* non-linear shallow water code which includes Coriolis and frictional effects. The *SWAN* code is described in reference 1. The calculations were performed on 50 Mhz 486 personal computers with 16 megabytes of memory. The one minute grid of the Hawaiian island chain was 480 x 360 cells and the time step was 4 seconds. The half minute grid of the islands of Hawaii, Lanai to Oahu was 400 x 400 cells and the time step was 2 seconds. To obtain the maximum possible runup of the tsunami wave, a friction coefficient of zero was used.

In Figure 1 the 105 Ka Lanai tsunami wave propagation from the largest Alika Slide source is shown. The tsunami wave exhibits a localized peak as it approaches the island of Lanai on its southwestern shore. This peak is 1.5 times higher than the rest of the wave and results in a localized high runup about in the region of Lanai where the highest coral deposits are reported. The island of Lanai details are shown in Figure 2 with the highest flooding occurring on the southwestern shore with runups of 340 meters.

In Figure 3 the tsunami wave as a function of time at various locations south of the southwestern end of Lanai and on the island of Lanai are shown. The seven locations are shown by dots in the first frame with location 1 being furthest South and location 7 being the furthest North. The locations, their depths and the wave characteristics are described in Table 3.

Even with a landslide with double the likely volume of the Alika 2 slide, the maximum calculated tsunami runup is less than the observed 400 meter. The simple landslide model used in the numerical calculation is a serious limitation as is the use of a shallow water model to describe the tsunami wave generated from a depression and uplift of the water surface as discussed in reference 8. It is possible that the Alika 2 landslide was the source of the 105 Ka Lanai tsunami; however the large landslide volume required by the numerical model is far from conclusive. A full Navier-Stokes model of the tsunami wave formation and a more realistic model for the landslide is clearly required.

Acknowledgments

The authors acknowledge the contributions of Mr. George Curtis, Dr. Gus Furamoto, Dr. Doak Cox, Dr. Dennis Moore, Dr. James Moore, and Mr. David King. Mr. George Nabeshima developed the one minute grid of the Hawaiian Island topography used in this study.

REFERENCES

1. Charles L. Mader *Numerical Modeling of Water Waves*, University of California Press, Berkeley, California (1988).
2. George W. Moore and James G. Moore, "Large-scale Bedforms in Boulder Gravel Produced by Giant Waves in Hawaii", Geological Society of American Special Paper 229, pages 101-110 (1988).
3. J. G. Moore, D. A. Clague, R. T. Holcomb, P. W. Lipman, W. R. Normark, and M. E. Torresan, "Prodigious Submarine Landslides on the Hawaiian Ridge", *Journal of Geophysical Research*, Vol 94, pages 17,463-17,484 (1989).
4. James B. Moore and David A. Clague, "Volcano Growth and Evolution of the Island of Hawaii", *Geological Society of America Bulletin*, Vol 104, pages 1471-1484 (1992).
5. James G. Moore and Robert K. Mark, "Morphology of the Island of Hawaii", *GSA Today*, Vol 2, pages 257-262 (1992).
6. J. G. Moore, W. R. Normark, C. E. Gutmacher, "Major Landslides on the Submarine Flanks of Mauna Loa Volcano, Hawaii", *Landslide News*, No 6, pages 13-15, (1992).
7. Carl Johnson and David King, "Can a Landslide Generate a 1000-ft Tsunami in Hawaii?" Twelfth Big Island Science Conference, April 29-May 1, 1993.
8. Charles L. Mader, "A Landslide Model for the 1975 Hawaii Tsunami", *Science of Tsunami Hazards*, Vol 2, pages 79-94 (1984).

TABLE 1
Lanai Slide Tsunami

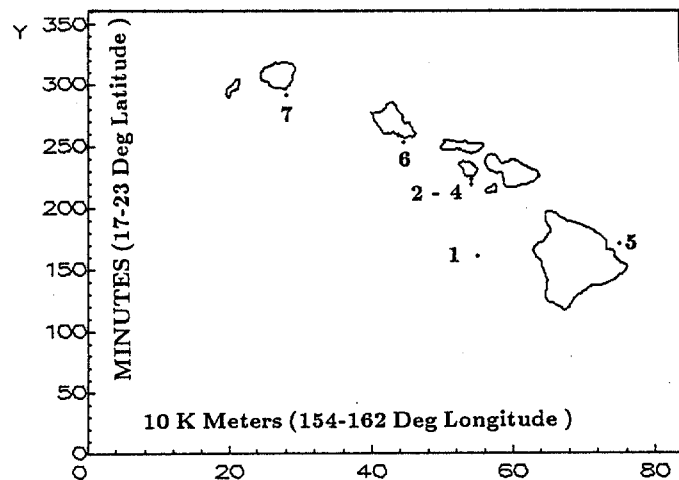
Location	Depth Meters	Lowest Amplitude Meters	Highest Amplitude Meters	Period Seconds
10x50x2 km Drop; 20x50x1 km Uplift				
1 Source	4549	-105	+80	100
2 Lanai	266	-40	+60	300
3 Lanai	166	-40	+25	350
4 Kahoolawe	261	-95	+95	300
5 Hilo	1373			
6 Honolulu	124	-120	+120	900
7 Lihue	890	-80	+80	350

TABLE 3
Alika Slide Tsunami (Half Minute Grid)

Location	Depth Meters	Lowest Amplitude Meters	Highest Amplitude Meters	Period Seconds
20x40x2 km Drop; 32x48x1 km Uplift				
1	3635	-260	+200	800
2	1835	-330	+230	800
3	337	-200	+260	1200
4	207	-200	+240	1500
5	105		+240	
6	-27		+340	
7	-3		+270	

TABLE 2
Alika Slide Tsunami

Location	Depth Meters	Lowest Amplitude Meters	Highest Amplitude Meters	Period Seconds
20x40x2 km Drop; 28x56x1 km Uplift				
1 Source	4549	-350	+440	400
2 Lanai	266	-140	+220	800
3 Lanai	166	-120	+190	1000
4 Lanai	149	-150	+190	900
5 Hilo	1373	-10	+10	800
6 Honolulu	124	-110	+125	1000
7 Lihue	890	-50	+50	500
20x20x2 km Drop; 28x28x1 km Uplift				
1 Source	4549	-260	+300	350
2 Lanai	266	-105	+160	600
3 Lanai	166	-110	+120	850
4 Lanai	149	-120	+130	800
5 Hilo	1373	-6	+6	700
6 Honolulu	124	-100	+80	800
7 Lihue	890	-40	+30	500
20x20x1.5 km Drop; 28x28x0.75 km Uplift				
1 Source	4549	-240	+220	350
2 Lanai	266	-90	+120	600
3 Lanai	166	-105	+100	800
4 Lanai	149	-100	+100	700
5 Hilo	1373	-5	+5	700
6 Honolulu	124	-90	+70	750
7 Lihue	890	-30	+20	500



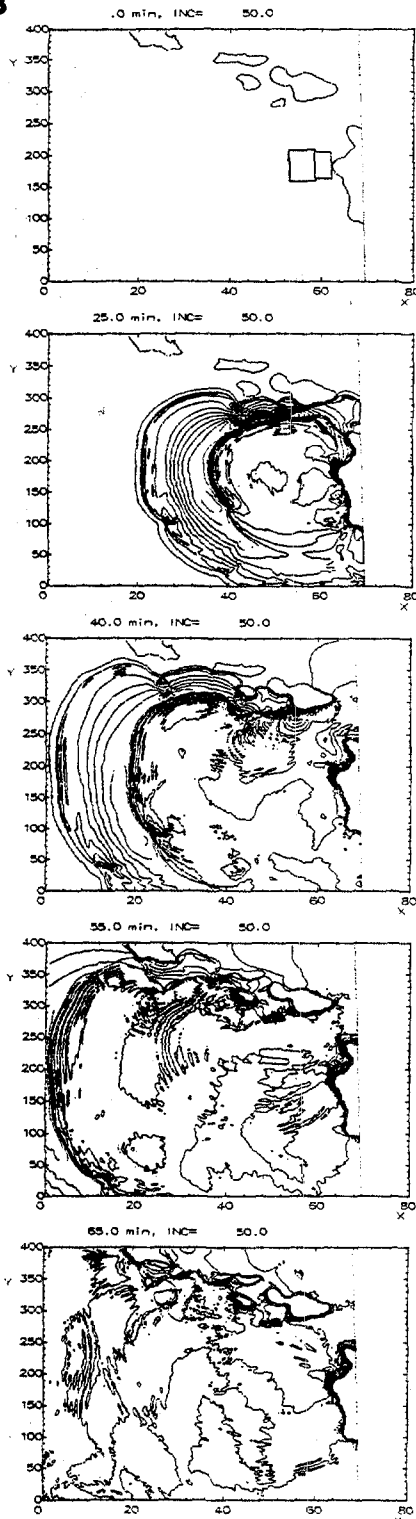


Figure 1.

The 105 Ka Lanai tsunami wave propagation from the Alika Slide source of a 20x40x2 kilometer drop and a 32x48x1 kilometer uplift. The contour interval is 50. meter, the mesh size is 0.5 minute with 400 by 400 cells.

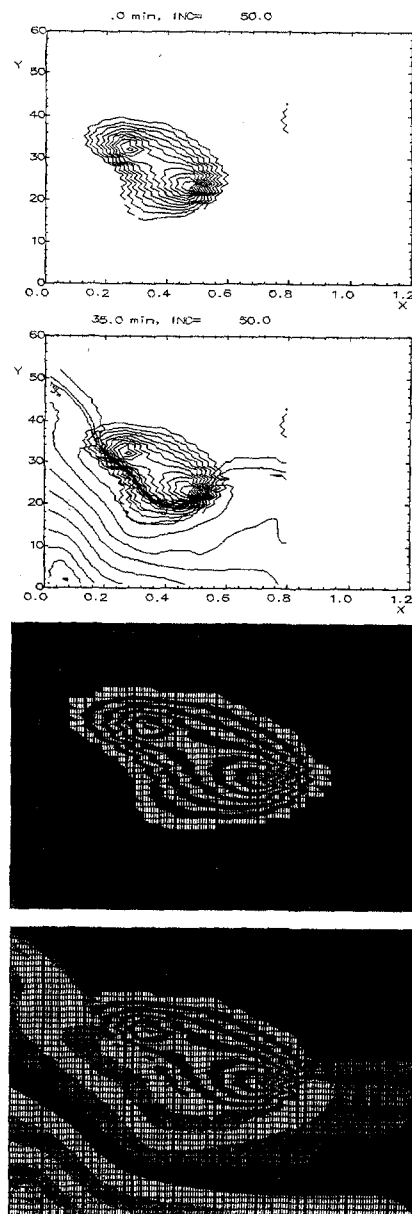


Figure 2.

The island of Lanai detail from the calculation shown in Figure 1. The land and water contour intervals are 50 meters. The contour plot is shown in a line and a picture plot. Flooding to over 300 meters occurs.

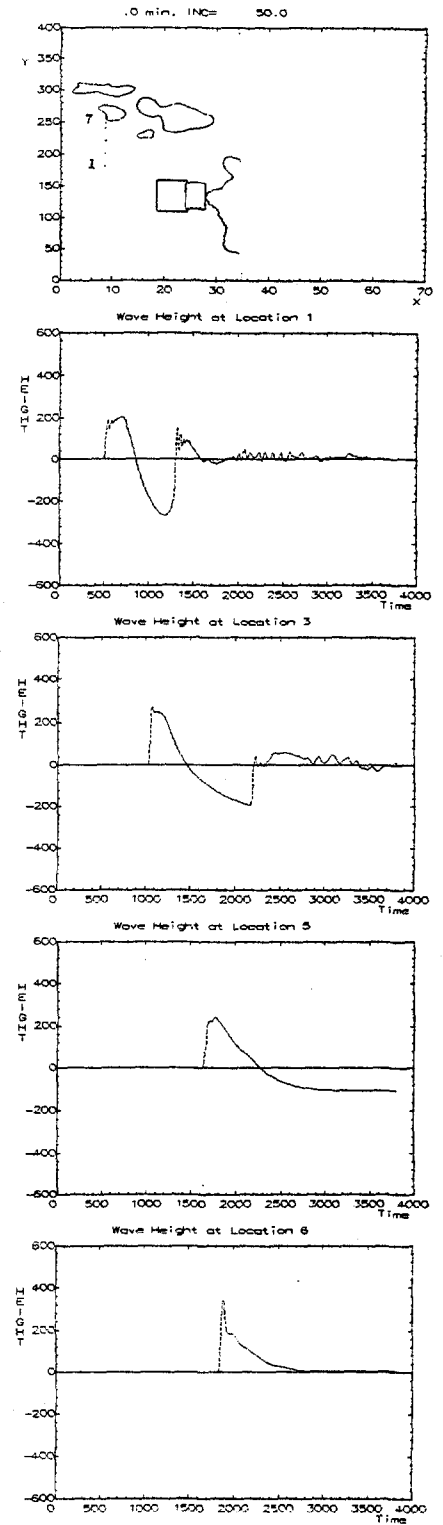


Figure 3.

The tsunami wave as a function of time at locations South of the island of Lanai in the ocean (Locations 1,3,5) and on land (location 6). The locations and wave characteristics are described in Table 3.

THE T-PHASE OF THE 1 APRIL 1946 ALEUTIAN ISLANDS TSUNAMI EARTHQUAKE

Daniel A. Walker
School of Ocean and Earth Science and Technology
Hawaii Institute of Geophysics and Planetology
University of Hawaii, Honolulu, HI, U.S.A.

Paul G. Okubo
U.S. Geological Survey
Hawaiian Volcano Observatory
Hawaii National Park, HI, U.S.A.

ABSTRACT

T-phases from historical earthquakes in close proximity to the 1 April 1946 Aleutian Islands tsunami earthquake recorded at the Hawaiian Volcano Observatory are examined and compared to the T-phase for the 1946 event. The T-phases examined from this region were generated by earthquakes with reported surface wave magnitudes ranging from 7.1 to 8.7 and occurred from 1917 to 1957. All data were taken from intermediate-period recordings on smoked paper. This system was in operation from 1913 through 1963. A comparison of T- to P-phase amplitude ratios for these earthquakes suggests that the T-phase for the 1946 event may be unusually large, implying that for so-called "tsunami earthquakes", tsunami amplitudes may be better correlated with T-phase amplitudes than with body or surface wave amplitudes.

INTRODUCTION

The Pacific-wide tsunami associated with the 1 April 1946 Aleutian Islands earthquake was one of the most devastating of the twentieth century. The 16.8 meter wave measured in Pololu Valley on the island of Hawaii is the highest value ever reported in the Hawaiian Islands for a Pacific-wide tsunami, and the value of 10.7 meters for the Hilo area (i.e., Onomea) is matched only by an identical value for the tsunami associated with the 23 May 1960 Chilean earthquake (Eaton et al., 1961). Kanamori (1972) compared different measures of earthquake strength derived from body and surface waves (i.e., body wave magnitudes, surface wave magnitudes, and seismic moments) to tsunami amplitudes and found the 1946 event to be quite anomalous. This discovery led to the identification of a special type of earthquake - the so-called "tsunami earthquake" for which tsunami amplitudes are much greater than would be expected from measures of the earthquake's seismic waves (Kanamori, 1972; Fukao, 1979). Of the handful of "tsunami earthquakes" reported in the literature (Kanamori, 1972; Fukao, 1979; Talandier and Okal, 1989; Satake and Kanamori, 1991), the 1946 Aleutian earthquake is the most significant in terms of the size of the tsunami generated and the discrepancy between the actual tsunami amplitude and the size of the earthquake inferred from seismic waves.

T-phases are hydroacoustic signals trapped in the SOFAR (Sound Fixing And Ranging) channel of the world's oceans. They are generated by earthquakes or explosions along the margins, or within the interiors, of oceans. They travel with little attenuation over thousands of kilometers, thereby providing unique information on the energetics of the water-sediment interface in the source area. Recent investigations of T-phases using deep-ocean hydrophones and high-quality digital tape recordings indicate that the T-phase spectral strength at frequencies from 10-35 Hz is closely correlated with seismic moment (Walker et al., 1992; Hiyoshi et al., 1992). Additional studies (Walker and Bernard, 1993) also suggest that T-phases may on some occasions be better indicators of tsunamigenesis than seismic moments. These findings are important because seismic moment has been thought to be a more reliable indicator of tsunamigenesis than body wave magnitudes or surface wave magnitudes (Kanamori, 1972; Abe, 1973; Okal and Talandier, 1986). Therefore, T-phases recorded on hydrophones could provide rapid, single station estimates of seismic moments and lead to advanced warnings related to

tsunami hazards. Unfortunately, "tsunami earthquakes" prove that seismic moments are not always reliable indicators of tsunamigenesis. Therefore, a remaining question is whether the T-phase strength for "tsunami earthquakes" correlates well with the seismic moment or is unusually large like the tsunami itself.

It is well established that seismic stations on islands are quite responsive to T-phases (e.g., Eaton et al., 1961; Talandier and Okal, 1979; Okal and Talandier 1986; Koyanagi, 1991). Especially relevant are the investigations of Eaton et al. and Koyanagi. Eaton et al. discuss the T-phase from the 1960 Chilean earthquake which was well-recorded by short period seismometers of the Hawaiian Volcano Observatory (HVO). Koyanagi uses T-phases recorded at different sites on the island of Hawaii from earthquakes in Alaska and California to determine variations in the structure of the island.

DATA

Because the island of Hawaii has an established responsiveness to T-phases from large earthquakes, we initially sought a T-phase recording from the 1946 Aleutian tsunami earthquake. The T-phase was found at its expected arrival time on the only recording available for that day - from a Bosch-Omori intermediate-period seismometer in the Whitney Vault on the rim of Kilauea Crater with a natural period of about 8 seconds (Klein and Koyanagi, 1980). Tracings of this phase from the original smoked paper record are shown in Figure 1.

This smoked paper recording format is capable of providing extremely fine recordings of small signals. The stylus scraping the soot from the chart paper has a diameter of approximately 0.1 mm. This fine resolution was especially useful for recording the high frequency signals from local earthquakes beneath Hawaii and it proved to be critically important in the registration of teleseismic T-phases. The T-phase from the 1946 Aleutian earthquake is monotonic with a predominant frequency of about 1 Hz. The T-phase amplitude builds and dies off gradually, and the duration of the phase is greater than 2 minutes. The most intense portion of this T-phase is shown in Figure 1. The T-phase is the high-frequency (1 Hz) energy superimposed on the longer period surface waves.

Having found the record from 1946, we then sought records from other Aleutian earthquakes registered on the HVO network. Because the Bosch-Omori smoked paper system was operated from 1913 through 1963, we restricted our search to that period, for events with roughly comparable or larger surface waves. This set a threshold at the equivalent of $M_s > 7.0$. To eliminate effects that might result from differences in source region and travel path, only those events located within 10° of longitude from the 1946 Aleutian tsunami earthquake were included. In addition, to further avoid complications arising from strongly azimuthally-dependent attenuation of converted T-phase energy near Hawaii (Koyanagi, 1991; Koyanagi et al., 1991), only those records from stations located at the summit of Kilauea Volcano were included.

Such azimuthally dependent attenuation may be due to differences in structure and to differences in the lengths of paths for the converted T-phases. For example, travel paths from the region of the 1946 earthquake of Kilauea Volcano will pass under much of the Island of Hawaii at an azimuth of about 10° east of due south, while travel paths from central or southern Alaska, will pass under a smaller and different portion of the island. Conversions from T-phases to ground phases are dependent on bathymetry and will occur at the intersection of the SOFAR (sound fixing and ranging) channel with the sloping seafloor.

A total of 14 earthquakes of magnitudes $M_s > 7.0$ were identified from an epicentral region extending from 153.5° to 173.5° W and 50° N to 60° N. No records could be located at HVO for four of these - 1916, 1929, 1948, and 1951. Signals from an event in 1923 were recorded photographically rather than on smoked paper. The photographic record does not provide the same resolution as the smoked paper, so the T-phase from this 1923 event could not be identified. Epicentral parameters of the nine remaining events are listed in Table 1. Epicenters are plotted in Figure 2 and the P- and T-phases are shown in Figure 3. S-phases from these events were at best not apparent or otherwise poorly registered. The surface waves for these large earthquakes were impossible to follow with confidence because adjacent traces overwrote one another.

It should be noted that surface wave magnitudes computed prior to the installation of the World-Wide Network of Standard Seismographs in 1964 are somewhat unreliable. Recent recomputations of magnitudes for large earthquakes ($M_s \geq 7.0$) are provided by Pacheco and Sykes (1992). However, only five of the nine earthquakes in Table 1 were found in that listing. Their revised magnitudes and seismic moments are given in Figure 3. The data given in Table 1 are

taken from Duda (1965).

Because of the very fragile quality of the historic smoked paper records, all of the signal traces are reproduced from tracings of the original records. Reproductions of the original records were not considered to be a viable option - not only because of their fragile nature, but because we could find no reasonable process for making such copies. The original records themselves can only be read with some difficulty on a light table. For signals with periods of 1 s or more, the accuracy of the cycle-per-cycle tracings is good. The 2 Hz signals of T-phases recorded at 60 mm/s drum rates are difficult to trace from cycle to cycle, but the T-phase amplitude is relatively easy to trace. Higher frequencies recorded on shorter time scales (i.e., 17/05/31) are obvious but are virtually impossible to trace. These T-phases are indicated by a blurring of the traces on the original records at the expected arrival time of the T-phase.

For all but the 1917 event, recordings were available for both E-W and N-S components. For two of the events (10 November 1938 and 27 July 1944), the E-W component was obviously not functioning properly (flat traces with intermittent offsets) and for another (9 March 1957) the trace could not be seen on the E-W component because of insufficient smoking of portions of the record. The N-S component for the 1 April 1946 event appears to have large microseisms (T=3 sec) which make identification of the P-phase quite difficult.

"On the Bosch-Omori instrument at the Observatory, the first impulse of the preliminary wave was recorded at approximately 02 06 20 Hawaii Standard Time, the exact emergence being somewhat obscured by very strong microseismic motion caused by the heavy trade-wide surf which had prevailed for a number of days (Powers, 1946)."

The P- and T-phases for the 1 April 1946 earthquake are much clearer and have greater signal to noise ratios on the E-W component. For the four other events for which both horizontal components appear to have been functioning properly, two of the events have comparable signals on both components, one has a larger P on the N-S component, and the other has a larger P on the E-W component. Modern short-period instrumentation at HVO reveals that the converted T-phases actually have their greatest amplitudes on vertical component seismographs. Koyanagi's analysis (1991) of converted T-phases propagating across the island of Hawaii indicates that these phases are, in fact, S-waves. The azimuth of approach from the epicenters to HVO is about 10° east of due south. Shown in Figure 3 are the available E-W component recordings for

comparison with the 1 April 1946 E-W recording. The component used is indicated above each trace.

DISCUSSION

At periods between about 2 s and 7 s, most of the Aleutian earthquakes in Table 1 generated P-wave amplitudes which are greater than that of the 1946 event (Figure 3). In other words, the P-wave from the 1946 event is relatively weak. The only comparable low-amplitude P-arrival is from the 10 April 1957 earthquake. This 1957 event and the 9 March 1957 earthquake had T-phases that were too small to trace (i.e., ≤ 0.5 mm). No T-phases were observed by the Bosch-Omori seismographs at Kilauea for the events of 22 August 1940 and 19 April 1957.

In contrast, the T-phase for the 1946 Aleutian earthquake is prominent and is comparable to that from the 10 November 1938 ($M_s=8.7$) earthquake. Thus, from Figure 3, either the P-phase for the 1946 event is unusually small or the T-phase is unusually large. The T- to P-amplitude ratios, as determined from the maximum peak-to-peak amplitudes in the T- and P-phase codas on the original recordings for all these earthquakes, are indicated in Figure 3. Note that the relatively large ratio for the 1946 Aleutian earthquake supports the suggestion that in comparing this event to other events, its T-phase amplitude, or its T- to P-amplitude ratio, is better correlated with its tsunami amplitude than with its P-wave amplitude. T- to P-amplitude ratios may prove to be especially useful indicators of tsunamigenic potential. Earthquakes with abnormally small P-phases generally have very shallow focal depths, and large T-phases are produced by high-frequency, long-duration vibrations at the base of the water column in the source area. Both of these factors may be of critical importance in the generation of tsunamis.

Of the events in Table 1 other than the 1946 earthquake, only the large 10 November 1938 earthquake is reported to have generated a Pacific-wide tsunami (0.3 m at Hilo, Hawaii; Iida et al., 1967). However, with modern instrumentation, Pacific-wide or regional tsunamis might have been detected for many of these earthquakes. It should once again be noted that due to uncertainties regarding instrument responses, conclusions based on the absolute amplitudes of either P-phases or T-phases may not be as reliable as conclusions based only on the comparisons of the T- to P-amplitudes ratios. Also, this information is itself incomplete because of the known

strength of the T-phase at frequencies much greater than 2 Hz (e.g., small changes in T- to P-amplitude ratios at T-frequencies of 1-2 Hz might imply much greater changes for higher frequencies of T).

We recognize that an important consideration is the actual magnification of the instruments for each of the records shown in Figure 3. Unfortunately, no gain levels were indicated on the recordings and no daily station logs could be found. Given the nature of seismic station operations and maintenance during the first half of this century, an assumption that the responses remained constant from 1917 through 1957 would be unrealistic. This is confirmed by Apple (1987).

"Fine tunings of the Bosch-Omori never ended and were required after almost every unhinging caused by a strong earthquake. Modifications and upgradings were intermittent: steel wire replaced silk fibers to suspend the weights; oil damping baths were added, adjusted, redesigned, and readjusted; friction reduction was tried; new hinges were designed and manufactured; magnifications were lowered and raised; different levers, recording pens, and pins were tried; timing devices were improved; better drum-smoking devices were found; Dr. Romberg modified linkages and levers in 1918 so that one smoked drum recorded what two drums did originally; and one of the piers was rotated 7.5° to permit its boom to swing closer to a true east-west line."

In this study the comparison of T- to P-amplitude ratios may be one method for reducing possible errors in interpretation due to possible changes in the magnification of the instruments. Such problems, of course, are minimized with well-calibrated, modern digital networks which also provide opportunities for spectral studies over a broad range of frequencies.

Slight changes in magnification or other instrumental characteristics, or variations in noise levels could explain any no T-phase was observed in California for the 1946 earthquake (Ewing, Tolstoy, and Press; 1950). On continental stations, T-phases are only marginally observed for only the largest of earthquakes, and noise levels can change dramatically when storms strike continental margins even hundreds of kilometers away. Much of this noise is in the same frequency range (1 to 2 Hz) at which T-phases are observed by conventional short-period seismometers.

Source mechanisms must also be considered in discussing tsunamigenesis. Possible mechanisms for the 1946 "tsunami earthquake" are discussed by Kanamori (1972) and, more recently, by Pelayo and Wiens (1991). Also, the 1917 earthquake is discussed in a recent

publication where its M_s has been revised to 7.4 ± 0.3 (Estabrook and Boyd, 1992). It is unlikely that many mechanisms are available for the other "conventional" earthquakes in Table 1. [None were found in searches of indexes for the Bulletin of the Seismological Society of America.] Source mechanism, however, may not be a significant factor in tsunamigenesis by conventional earthquakes. Okal (1988) and Talandier and Okal (1989) found no apparent correlation between tsunami wave heights and source mechanisms for conventional earthquakes, nor are any correlations apparent for the source mechanisms of such earthquakes and their T-phase spectral strengths (Walker et al., 1992; Hiyoshi et al., 1992).

Finally, it should be noted that the 9 March 1957 earthquake is an aftershock of a major tsunamigenic earthquake which occurred just outside of the area of interest. This main shock was located at 51.63°N , 175.41°W with a surface wave magnitude of 8.1 and a seismic moment of $1.0 \times 10^{22} \text{Nm}$ (Pacheco and Sykes, 1992). The maximum runup reported in Hawaii for this event was 16.1 meters on the island of Kauai. Unfortunately, the pen of the Bosch-Omori instrument was broken by this earthquake before the T-phase could be recorded. The T-phase, was, however, recorded by other seismometers at Kilauea. A maximum amplitude of 7mm was found on a short-period vertical seismometer. This is not surprising since the peak frequency of T-phases is well in excess of 1Hz, with frequencies as high as 40Hz observed on SOFAR hydrophones for teleseismic earthquakes. However, since the only known T-phase recording of the 1946 "tsunami earthquake" is on an intermediate-period Bosch-Omori seismometer, the significance of this T-phase can only be examined by comparisons to similarly recorded T-phases for similar travel paths, and not to T-phases recorded by short-period seismometers or hydrophones. This is especially true since the interrelationships between these differing instruments is unknown and reliable calibration data for the older Hawaiian Volcano Observatory seismographs is not available.

CONCLUDING REMARKS

This report examines what may be the only known T-phase recording of the 1 April 1946 Aleutian Islands "tsunami earthquake" which produced one of the largest tsunamis in this century. Also of historical significance is the discovery of the earliest known, instrumentally recorded T-

phase (31 May 1917). These events and others examined in this study were recorded at the Hawaiian Volcano Observatory which began operation in 1912. Although no data are available for the 1946 Aleutian Island earthquake for those frequencies at which T-phases have been observed to have their greatest strengths on ocean hydrophones (i.e., >2 Hz), we can conclude that this T-phase, at frequencies of 1-2 Hz, is unusually large relative to its P-phase when compared to the T- and P-phases of other earthquakes from the same location with comparable or larger magnitudes. This finding supports the contention that T-phase strengths or T- to P-phase amplitude ratios may be better correlated with tsunami wave heights than with surface wave magnitudes or seismic moments for "tsunami earthquakes" (i.e., those earthquakes having tsunamis which are larger than would be predicted from their seismic waves). Such a finding, if confirmed with additional data, would provide for substantial, necessary improvements in the reliability of tsunami warning systems.

ACKNOWLEDGEMENTS

We thank all those past and present at HVO whose efforts resulted in the recording and archiving of unique, invaluable data for so many decades. We especially recognize Bob Koyanagi for his dedication to this archive. We thank Bob Koyanagi and Jerry Eaton for reviewing this report. This research was supported by the U.S. National Weather Service - Pacific Region, the Pacific Tsunami Warning Center, and NOAA's Pacific Marine Environmental Laboratory. School of Ocean and Earth Science and Technology contribution 3602, Hawaii Institute of Geophysics and Planetology contribution number 773 and Joint Institute for Marine and Atmospheric Research contribution 94-275.

REFERENCES

- Abe, K. (1973). Tsunami and mechanisms of great earthquakes, Phys. Earth Planet. Inter. 7, 143-153.
- Apple, R.A. (1987). Thomas A. Jaggar, Jr., and the Hawaiian Volcano Observatory, in Volcanism in Hawaii, U.S. Geol. Surv. Prof. Pap. 1350, edited by R.W. Decker, T.L. Wright, and P.H. Stauffer.
- Duda, S. (1965). Secular seismic energy release in the circum-Pacific belt, Tectonophysics 2, 409-452.
- Eaton, J.P., D.H. Richter, and W.U. Ault (1961). The tsunami of May 23, 1960, on the island of Hawaii, Bull. Seismol. Soc. Am. 51, 135-157.
- Estabrook, C.H., and T.M. Boyd (1992). The Shumagin Islands, Alaska, earthquake of 31 May 1917, Bull. Seismol. Soc. Am. 82, 755-773.
- Ewing, M., I. Tolstoy, and F. Press (1950). Proposed use of the T-phase in tsunami warning systems, Bull. Seismol. Soc. Am. 40, 53-58.
- Fukao, Y. (1979). Tsunami earthquakes and subduction processes near deep-sea trenches, J. Geophys. Res. 84, 2303-2314.
- Gutenberg, B. and C.F. Richter (1965). Seismicity of the Earth, Hafner Publishing Co., New York, 310p.
- Hiyoshi, Y., D.A. Walker, and C.S. McCreery (1992). T-phase data and regional tsunamigenesis in Japan, Bull. Seismol. Soc. Am. 82, 2213-2223.
- Iida, K., D.C. Cox, and G. Pararas-Carayannis (1967). Preliminary catalog of tsunamis occurring in the Pacific Ocean, Hawaii Inst. of Geophysics Rept. 67-10, unpagged.
- Kanamori, H. (1972). Mechanism of tsunami earthquakes, Phys. Earth Planet. Inter. 6, 346-359.
- Klein, F.W. and R.Y. Koyanagi (1980). Hawaiian Volcano Observatory seismic network history 1950-79, U.S. Geol. Surv. Open File Rep., 80-302.
- Koyanagi, S.K. (1991). Determination of coda site amplification factors and inferred attenuation from T-phases on the island of Hawaii, Thesis - Univ. of Southern California, 109pp.
- Koyanagi, S., K. Mayeda, and K. Aki (1991). Site-effect corrected T-phase amplitudes and inferred attenuation in the Kilauea Volcano region, island of Hawaii, Eos, Trans. Amer. Geophys. Un. 72, 198-199.
- Okal, E.A. (1988). Seismic parameters controlling far-field tsunami amplitudes: a review, Natural Hazards Journal, 1, 69-96.

- Okal, E.A. and J. Talandier (1986). T-wave duration, magnitudes and seismic moment of an earthquake - application to tsunami warning, J. Phys. Earth, 34, 19-42.
- Pacheco, J.F. and L. R. Sykes (1992). Seismic moment catalog of large, shallow earthquakes, 1900-1989, Bull. Seismol. Soc. Am. 82, 1306-1349.
- Pelayo, A.M. and D.A. Wiens (1991). The April 1, 1946 Aleutian tsunami earthquake: the largest known slow seismic event, Eos, Trans. Amer. Geophys. Un. 72, 292-293.
- Powers, H.A. (1946). The tidal wave of April 1, 1946, The Volcano Letter 491, 6pp.
- Satake, K. and H. Kanamori (1991). Abnormal tsunamis caused by the June 13, 1984, Torishima Japan, Earthquake, J. Geophys. Res. 96, 19,933-19,939.
- Talandier, J. and E.A. Okal (1979). Human perception of T-waves: the June 22, 1977 Tonga earthquake felt on Tahiti, Bull. Seismol. Soc. Am. 69, 1475-1486.
- Talandier, J. and E.A. Okal (1989). An algorithm for automated tsunami warning in French Polynesia based on mantle magnitudes, Bull. Seismol. Soc. Am. 79, 1177-1193.
- Walker, D.A. and E.N. Bernard (1993). Comparison of T-phase spectra and tsunami amplitudes for tsunamigenic and other earthquakes, J. Geophys. Res. 98, 12,557-12,565.
- Walker, D.A., C.S. McCreery, and Y. Hiyoshi (1992). T-phase spectra, seismic moments, and tsunamigenesis, Bull. Seismol. Soc. Am. 82, 1275-1305.

TABLE 1

Large Earthquakes from the Aleutian Islands Near 163.5°W Recorded by the Hawaiian Volcano Observatory¹

No.	Origin Time		Coordinates		Depth (km)	Ms
	yr/mo/day	hr/min/sec	°N	°W		
1	17/05/31	08 47 20	54.5	160.0	s ²	7.8
2	38/11/10	20 18 43	55.5	158.0	s	8.7
3	38/11/17	03 54 34	55.5	158.5	s	7.2
4	40/08/22	03 27 18	53.0	165.5	s	7.1
5	44/07/27	00 04 23	54.0	165.5	70	7.1
6	46/04/01	12 28 54	52.8	163.5	s	7.4
7	57/03/09	20 39 15	52.5	169.5	s	7.1
8	57/04/10	11 29 58	56.0	154.0	s	7.1
9	57/04/19	22 19 26	52.0	166.5	50	7.3

¹ Epicenter data taken from Duda (1965).

² Shallow depth.

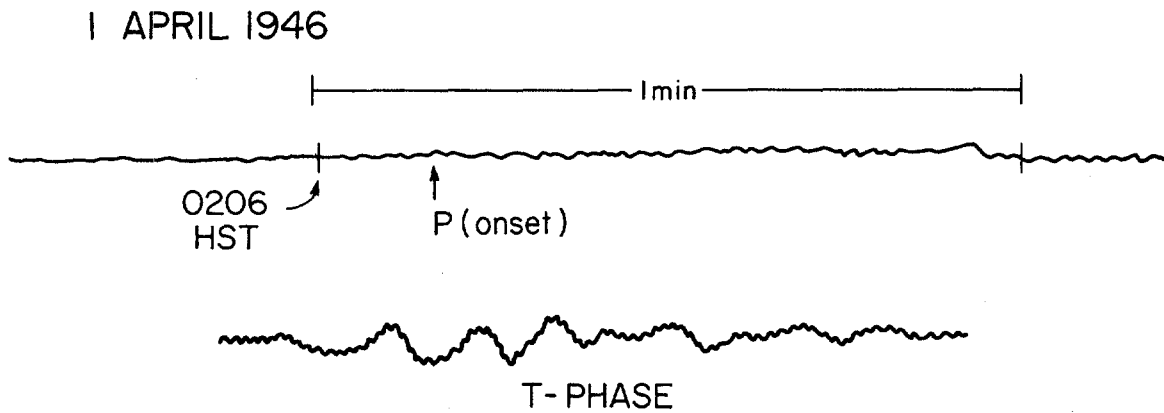


Fig. 1. Recording of the 1 April 1946 Aleutian Islands earthquake at the Hawaiian Volcano Observatory on a Bosch-Omori intermediate-period seismograph. The T-phase is indicated by the higher frequency (1Hz) oscillations superimposed on the longer period (6 sec) surface waves of the 1 April 1946 earthquake. Note that the T-phase, which travels with a velocity of about 1.5 km/sec, is recorded long after the P-arrival. Thus, in this figure and in Figure 3, recordings shown are only segments of the total records.

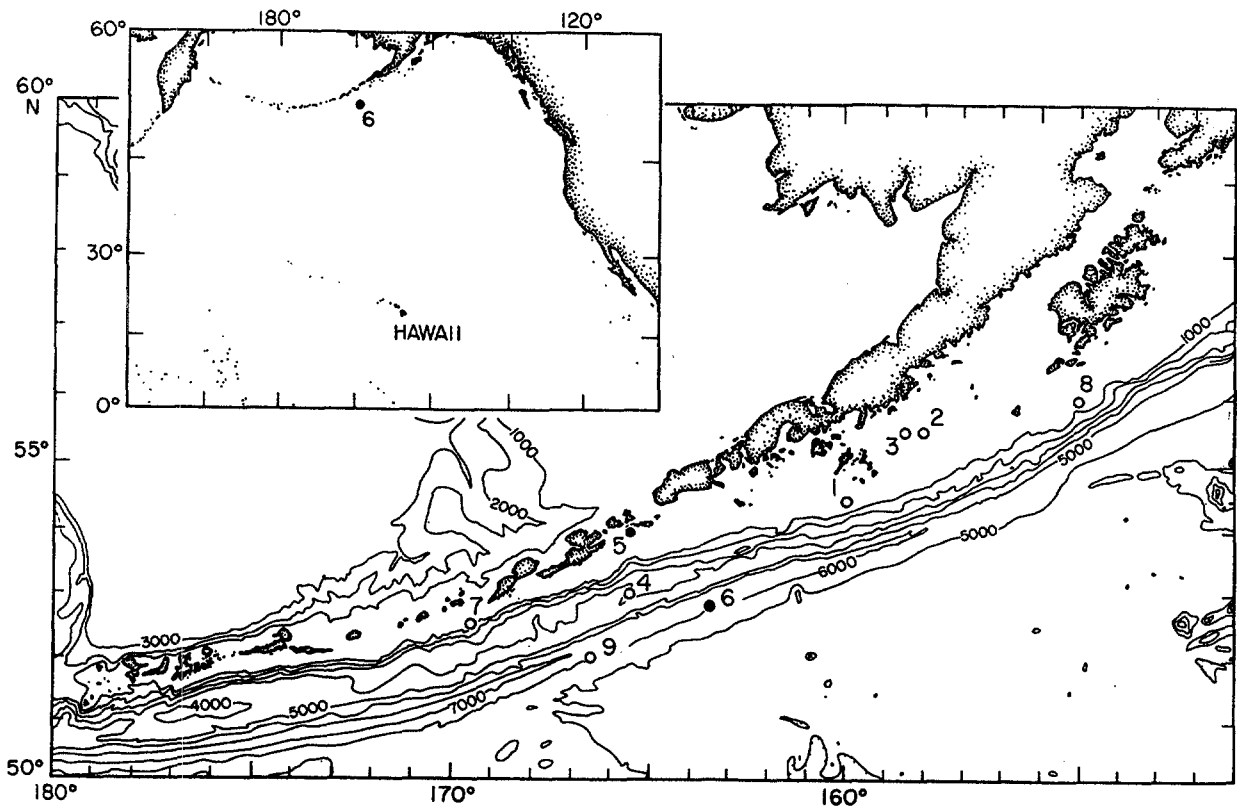


Fig. 2. Locations of earthquakes used in this study for comparisons of P- and T-phase amplitudes to the 1 April 1946 earthquake (no. 6). Depths are in meters.

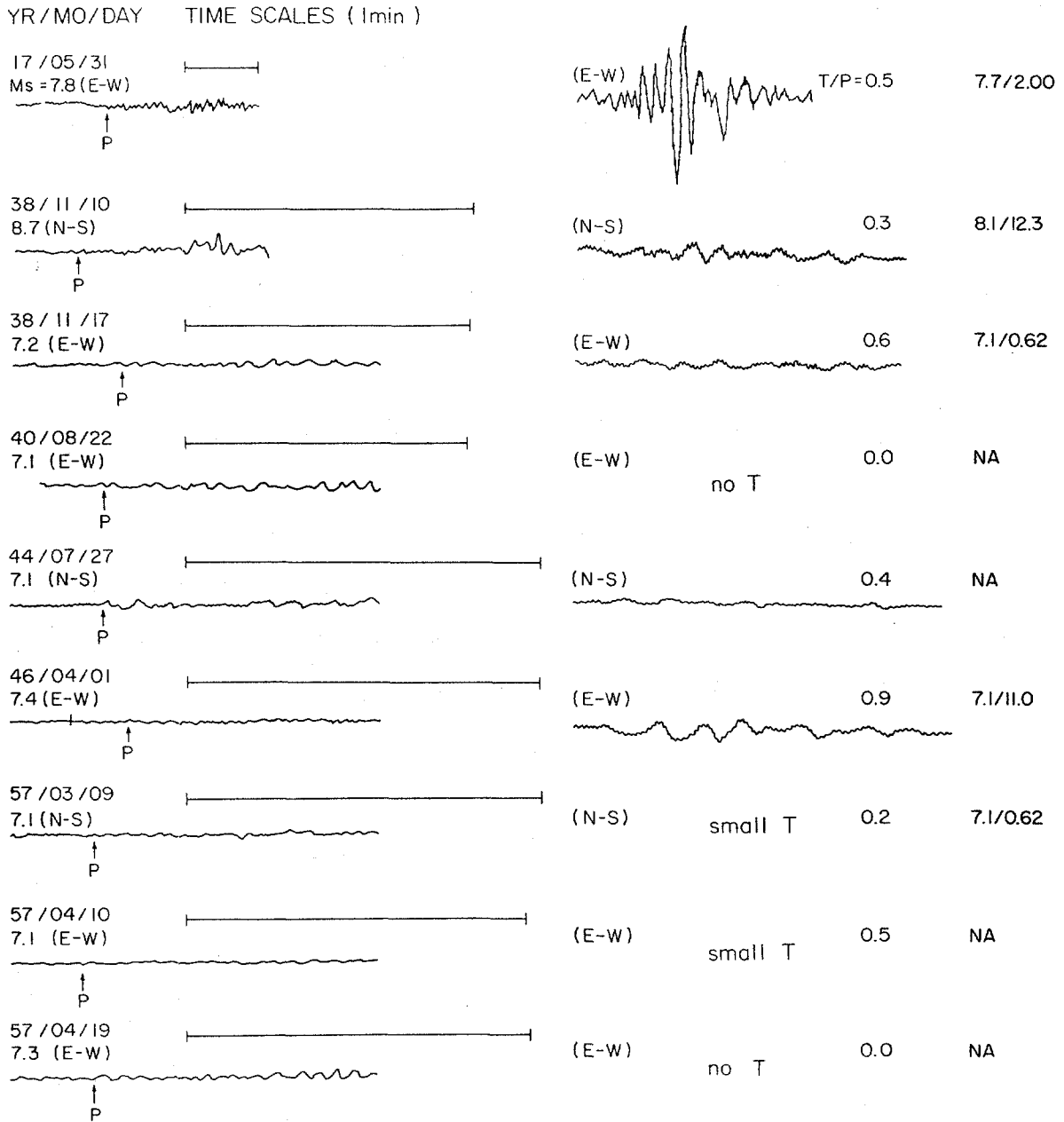


Fig. 3. P- and T-phases for earthquakes listed in Table 1 and shown in Figure 2. All phases were recorded by the Bosch-Omori horizontal seismographs located near the summit of Kilauea on the island of Hawaii. The E-W component was used wherever possible for comparison with the E-W recording of the 1 April 1946 event. Again, the T-phase is indicated by the shorter period oscillations superimposed on the longer period surface waves for those earthquakes. The T- to P-amplitude ratios were based on actual measures of the signals on the original recordings (see text for further discussions). Surface wave magnitudes indicated along the left hand margin are those taken from Duda (1965). Surface wave magnitudes and seismic moments in 10^{20} Nm from Pacheco and Sykes (1992) are indicated along the right hand margin. NA - not available.



PROPOSED: A Hilo Tsunami Museum to respond to high community and visitor interest and achieve the following critical goals:

- (1) Promote Public Education
- (2) Support Safety/Warning Systems
- (3) Preserve Local History
- (4) Foster Community Development
- (5) Expand Hilo Economic Activity
- (6) Promote International Study

The expected visitor profile would likely exceed 75,000 visitors per year, including tourists and local programming. An entry fee of \$5 would generate \$375,000 per year. This is a modest estimate given the one million visitors annually to Hawaii Volcanoes National Park.

EXHIBITS AND PROGRAMS:

- 3 permanent exhibits on Tsunami history, nature, impact, and public safety: (1) What they are! (2) How they've hit! (3) What's next and what to do!
- Emphasis on realism: working sensors tied into island system; touch-sensitive monitor display; videos; maps; "make your own" interactive computer display;
- "Talk story" living history and current research program
- Tsunami Theater to feature custom-made 3-D tsunami experience film, public lectures, tsunami cultural activities

COMPLETION: April 1, 1996

(50th Anniversary of the 1946 Hilo tsunami)

SITE AND DESIGN OBJECTIVES:

- Existing building in the heart of downtown Hilo;
- Maximum accessibility for all visitors, including foreign language;
- 2,500 square feet permanent exhibit space;
- 600 square feet "talk story" space;
- Tsunami Theater for minimum 75 persons;
- Classroom for minimum 30.

Join the Friends of the Hilo Tsunami Museum!

Tsunami! The word sparks the imagination--a phenomenon of nature, a scientific challenge, a human drama. Tsunamis are a fact of life in Hawaii, especially in Hilo which has been ravaged far worse than anywhere else in the islands. We cannot ignore these catastrophic waves but must learn to live with them and prepare for the next tsunami. Tsunami specialist Dan Walker has stated that "the people of Hawaii, including public officials, may have been lulled into a false sense of complacency regarding the danger and frequency of tsunamis, and possibly a false sense of security and confidence in the ability of warning systems to predict tsunamis."

One reason for complacency has been that for almost 30 years there have been no large tsunamis to strike the Hawaiian Islands. During this same period, Hawaii has experienced enormous growth of both resident and visitor populations, but less than half of our resident population and virtually none of the visitors to Hawaii has had any experience with tsunami hazards. Tsunami education can be delivered in an effective, non-threatening way to the community, visitors, and local school children. Furthermore, a *Hilo Tsunami Museum* would preserve local history, and be a much-needed added visitor attraction for Hilo.

Many survivors of the 1946 and 1960 tsunamis still reside within the state of Hawaii. Oral histories, along with scientific information would serve as the data base for the interpretation at the *Hilo Tsunami Museum*. Permanent exhibits would interpret what the tsunami phenomenon, history and impact using Hilo as an example, and provide safety information. Visitor demand for interpretation and requests for tsunami memorabilia (books, post cards, T-shirts), already high, will be met by the new facility.

The *Hilo Tsunami Museum* is a non-profit organization under the auspices of the University of Hawaii Foundation. The museum will secure its initial funding through grants and private donations. After its grand opening in April of 1996, general operating support will be acquired through admission and gift shop revenue, membership drives, and rental of facilities.

We need your financial support **now**. Please join us and become a Charter member of the Friends of the *Hilo Tsunami Museum*. All gifts are tax deductible.

Checks should be made out to the UH Foundation and forwarded to Hilo Tsunami Museum, P.O. Box 806, Hilo, Hawaii 96720.

EFFECT OF THE NEXT DATA POINT ON TSUNAMI FLOOD LEVEL PREDICTION

Fred E. Camfield
Debra R. Green
U.S. Army Engineer Waterways Experiment Station
Coastal Engineering Research Center
Vicksburg, MS 39180-6199

ABSTRACT

Probabilities of occurrence for tsunami flood levels are obtained from statistical analysis of available data. Data sets may be limited both by the infrequent occurrence of tsunamis, and the possibility that some smaller tsunamis may have gone unrecorded. It is desirable to test statistical predictions to determine the magnitude of potential errors. Tests can be performed by adding random values to data sets to determine the sensitivity of the analysis to additional data.

INTRODUCTION

Tsunamis occur infrequently at most coastal points (Camfield, 1990). Statistical predictions of tsunami flood levels are commonly based on a limited number of data points from historic tsunamis (Camfield, 1987). These predictions are used for a variety of purposes including hazard mitigation planning, determination of tsunami evacuation zones, and requirements for flood insurance (Preuss, 1987). Consequently, an assessment needs to be made on the confidence levels of the predictions, and how additional data may affect the predicted flood levels.

Using a hypothetical data set, comparisons can be made of predictions based on different sets of data (Camfield, 1987). Using a relationship developed by Cox (1964), Houston, et al. (1977) showed a semi-logarithmic relationship for the probability of occurrence of tsunami flood levels. For earlier periods of record, smaller tsunamis may not have been noted and, therefore, would not have been recorded.

COMPARISON OF PREDICTIONS

Assume, for example, there is a 220 year period of record, and five recorded tsunamis had flood elevations of 5 m, 4.2 m, 3.5 m, 3.2 m, and 2.7 m. Ranking the tsunamis from the largest to the smallest would give probabilities of occurrence of 0.0045, 0.0090, 0.0136, 0.0181, and 0.0226 (Linsley, et al., 1958). Linear regression (Draper and Smith, 1966) will then give a relationship between the flood level, h , and the logarithm of the probability of occurrence in any year, $P(h)$, as shown in Figure 1. A 90 percent confidence limit on the prediction also can be obtained using the standard error and a t -distribution with two degrees of freedom (Draper and Smith 1966; Camfield 1981, 1987).

One can then explore the effect of adding an additional data point to the analysis. Assume at the end of the 220 year period of record, a minor tsunami occurs producing a flood elevation of 0.6 meters. This added data point then produces a new regression curve (Figure 1), and a new confidence limit on the predictions. It can be seen that adding a low flood level to a set of data comprised only of high flood levels will give a major difference in predicted values. In particular, the predicted flood levels for extreme events will become higher because of the change in slope of the regression line, while the predicted level of more frequent tsunamis will become lower. For the case illustrated, the confidence band also became wider.

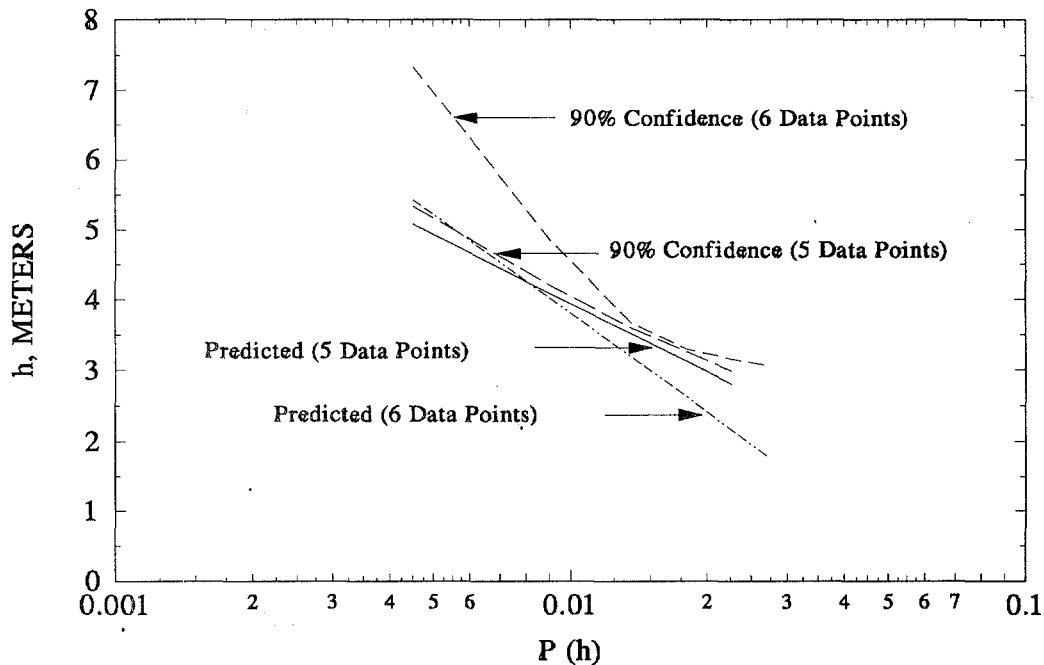


Figure 1 Effect of adding a low data point to a data set of high flood levels

Consider, next, a data set where records of some smaller tsunamis were included in the original record. For the hypothetical example, add events producing flood elevations of 1.2 meters and 0.5 meters to the original set of five flood levels. This produces the results shown

in Figure 2 for seven data points. It can be seen again that this will produce significantly different results than those obtained using only the five high flood levels (Figure 1). As before, inclusion of the lower flood levels in the analysis gives higher predicted flood levels for extreme events (Camfield, 1987). If one then includes the minor tsunami, 0.6 meter flood level, occurring at the end of the period of record, the second set of results in Figure 2 is obtained. It can be seen that the inclusion of this additional lower flood level has little effect on the predictions when the original data set includes data with similar lower values. Comparing the results shown in Figures 1 and 2, it is interesting to note that the addition of one, two, or three lower values produces only minor differences in the prediction of extreme flood levels.

Next consider the case of a large tsunami occurring at the end of the period of record. Add a tsunami flood level of 5.1 meters to the example data set. Added to the five high data

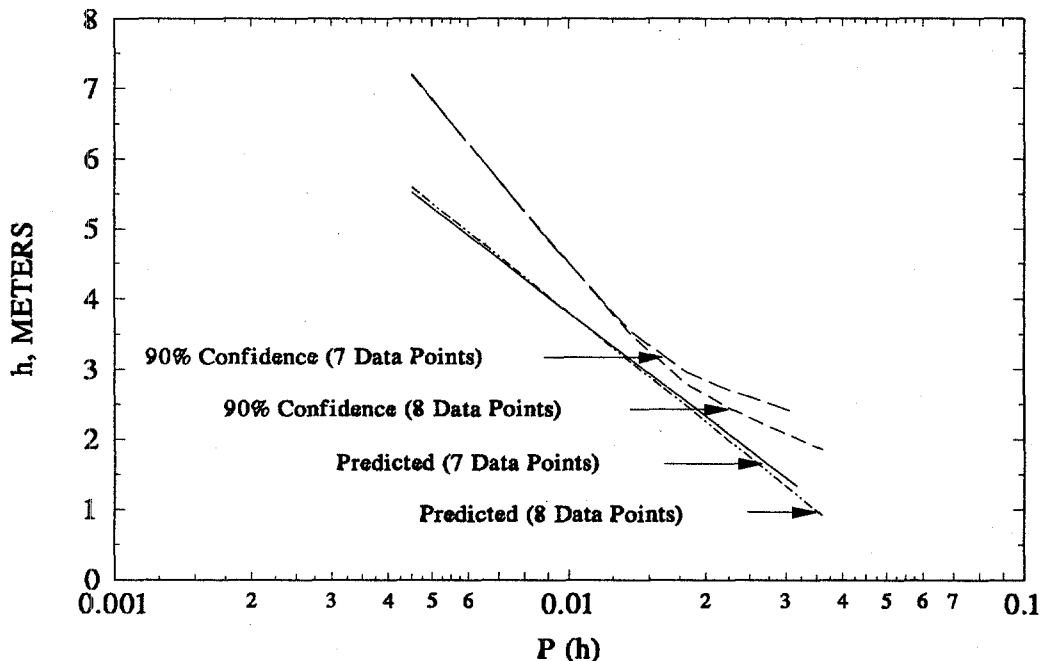


Figure 2 Effect of adding multiple low data points to a data set of high flood levels

points, the additional high flood level will cause some shift in the regression curve (Figure 3), but this shift tends to be somewhat uniform for all probabilities of occurrence, i. e., there is not a major change in the slope of the regression line.

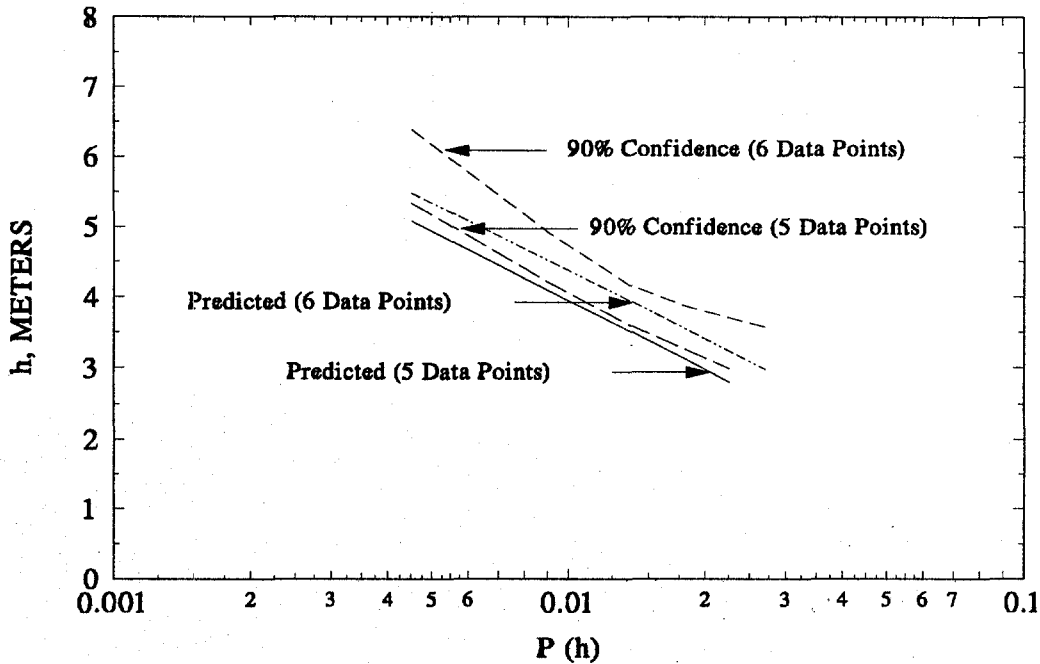


Figure 3 Effect of adding a high data point to a data set of high flood levels

If the additional high flood level is added to the set of seven data points, including the two lower points, the result is shown in Figure 4. Again, there is a somewhat uniform shift in the regression line, but no major change in slope, i.e., predicted flood levels become somewhat higher for all probabilities of occurrence.

DISCUSSION AND CONCLUSIONS

Predictions of the probability of occurrence of various tsunami flood levels at a particular coastal point are based on a statistical analysis of the available data at that point. The confidence

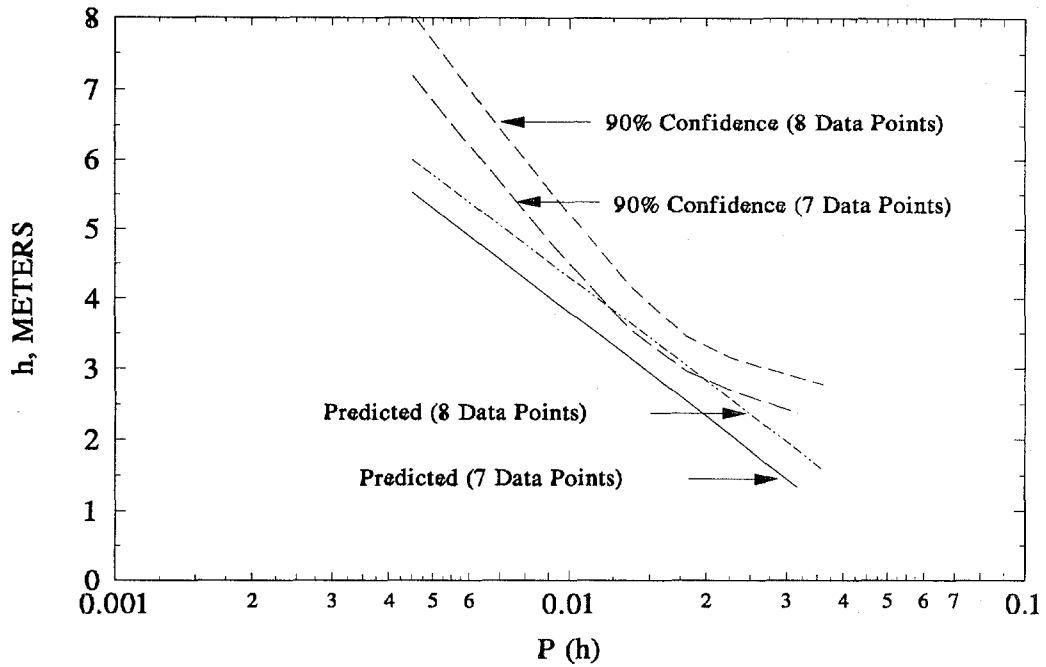


Figure 4 Effect of adding a high data point to a data set of high and low flood levels

bands on a regression curve give some indication of the reliability of the predictions. In addition, some error may be present in the predictions because of unrecorded data, i.e., smaller tsunamis. As tsunamis are random events, statistical predictions will change as additional tsunamis occur.

The inclusion of a single small tsunami in a data set of larger tsunamis can significantly alter predictions. It is desirable, then, to test the possible change in predictions. Predictions obtained from regression analyses can be tested by incorporating random values into the data. Examples of single or multiple data points can be incorporated into the analysis to examine possible changes in the predictions.

Likewise, results can be tested by incorporating an additional data point for a high flood level. Testing results by adding additional example data points and calculating confidence bands will give some indication of the degree of potential error in the statistical predictions.

ACKNOWLEDGEMENT

This paper was prepared under the Coastal Engineering Research Program of the U.S. Army Corps of Engineers Civil Works Research Program at the U.S. Army Engineer Waterways Experiment Station, Coastal Engineering Research Center. Permission of the Chief of Engineers to present and publish this paper is appreciated.

REFERENCES

Camfield, F. E., "Confidence Limits on Predicted Values," Coastal Engineering Technical Note I-3, U. S. Army Engineer Waterways Experiment Station, Vicksburg, Mississippi, Jan. 1981.

Camfield, F. E., "Insufficient Data Effects on Tsunami Flood Level Predictions - Summary," Proceedings, International Tsunami Symposium, Pacific Marine Environmental Laboratory, NOAA, Contribution No. 1041, pp. 247-251, 1987.

Camfield, F. E., "Tsunami," in Herbich, J. B. (ed.), Handbook of Coastal and Ocean Engineering, Vol. 1, Wave Phenomena and Coastal Structures, Gulf Publishing Co., Chapter 10, pp. 591-634, 1990.

Cox, D. C., "Tsunami Height-Frequency Relationship of Hilo," unpublished paper, Hawaii Institute of Geophysics, University of Hawaii, Honolulu, Hawaii, Nov. 1964.

Draper, N. R., and H. Smith, Applied Regression Analysis, John Wiley and Sons, Inc., New York, 1966.

Houston, J. R., R. D. Carver, and D. G. Markle, "Tsunami-Wave Elevation Frequency of Occurrence for the Hawaiian Islands," Technical Report H-77-16, U.S. Army Engineer Waterways Experiment Station, Vicksburg, Mississippi, Aug. 1977.

Linsley, R. K., Jr., M. A. Kohler, and J. L. H. Paulhus, Hydrology for Engineers, McGraw-Hill Book Company, New York, 1958.

Preuss, J., "Tsunami Hazard Reduction Through Risk Mitigation," Proceedings, International Tsunami Symposium, Pacific Marine Environmental Laboratory, NOAA, Contribution No. 1041, pp. 263-275, 1987.

MEMORIUM

Professor Sergei Soloviev

Professor Sergei Soloviev was born on April 12, 1930 in the ancient Russian city of Novgorod, 150 km from Leningrad (now St. Petersburg). He attended secondary school there but in 1941 had to evacuate to Kostroma due to the German invasion. In 1947 he was able to finish secondary school in Leningrad with the gold medal award, and began the study of physics at Leningrad University. He specialized in geophysics and became especially interested in the problems of observational seismology. He graduated from the University in 1953 and continued his education with postgraduate courses at the Geophysical Institute (now the Institute of Physics of the Earth) in Moscow. There he was student of Professor E. Savarensky, a leading Russian seismologist, who was Director of the Moscow Seismological Observatory. As a main subject for his research work, Professor Savarensky proposed a serious (for the graduate student) task: to adjust the magnitude scale introduced by K. Richter and B. Gutenberg in the USA, for the regional earthquakes recorded in the U.S.S.R. In 1956, Sergei finished the graduate courses and defended his Master's thesis entitled "Magnitude Classification of the Earthquakes in the USSR". In the same year he became a junior researcher in the Institute. As a part time job he took a position of the Learned Secretary of the Seismological Council of the USSR Academy of Sciences and continued until 1961. His main work during this period of almost 5 years was editing the fundamental book prepared by the group of authors entitled "Atlas of the Earthquakes in the USSR". This book was the first attempt to collect the original observational data on all historical earthquakes in Soviet territory and classify them on the basis of the unified magnitude scale. In 1961 he moved from Moscow to Sakhalin and took the position of Head of the Seismological Department of the Sakhalin Complex Research Institute (SCRI). Due to the geographical position of the institute near one of the most active segments of the Pacific "Ring of Fire", the tsunami problem inevitably became the focus of his attention. He helped established the Soviet Tsunami Warning System on the Far East coast, and proposed and elaborated a set of magnitude criteria for issuing the tsunami warnings, participated in the field investigation of both 1963 tsunamis on the Urup Island, the second of which was the largest in this area after the 1952 Great Kamchatka tsunami. He established the Hydrophysical Observatory on Shikotan Island where the experimental works on T-phase observations and the direct bottom measurements of tsunami by cable sensors started in 1963. Among the scope of his research work at that time was the investigation of seismicity of the Sakhalin which resulted in the publication of the first monograph on this subject. The compilation of observational data for the tsunami occurrence in the Pacific region was made during this period. Two volumes of the tsunami catalogs for the Pacific were published in Moscow in 1974-75 and later were translated into English. For a whole generation of tsunami researchers in the Soviet Union these books were the primary source of information for historical tsunami data. In 1965 Sergei Soloviev was appointed Deputy-director of the SCRI; however, in 1968 due to the illness of his daughter, he had to return to Moscow and during the next three years he again worked in the Institute of Physics of the Earth. There he prepared and in 1970 defended his PhD thesis entitled "Seismological Aspects of Tsunami Occurrence". In 1972 he was elected

as a Corresponding Member of the Academy of Sciences of the USSR. Soon after that he was invited back to Sakhalin and took the vacant position of Director of the SCRI. During the next several years he reactivated the institute and initiated several new projects. One of his primary concerns was the development of the research and technical basis of the Institute. As a result, the Institute obtained three research vessels Pegas, Sea Geophysics and Audacious and the intensive program of geophysical investigation of the Okhotsk and adjacent seas was started. In these years, the first steps in the Soviet-American cooperation in the field of tsunami research were taken. Professor Soloviev was at the forefront of these programs and actively supported all co-operative projects. He took part in the Washington (1974) and Novosibirsk (1976) USA-USSR meetings of experts on the tsunami problem and initiated two joint Soviet-American tsunami expeditions in the Kuril-Kamchatka region. His good command of the English language was revealed during these activities. In 1971 he was elected as Chairman of the IUGG Tsunami Commission and held this position till 1979 when some problems involving his trips abroad appeared from the the Foreign Department of the Academy of Sciences. However, in 1985, he attended the Tsunami Symposium in Victoria (Canada) where he was awarded by the special IUGG Memorial Plate for the active research in the field of tsunami problems. In 1988 he received the Adams Award in recognition of his long-term contributions in tsunami research. At the XI session of the ITSU Group in Beijing in 1987 Professor Soloviev was elected Vice-President of the Group. In 1977 Professor Soloviev returned to Moscow from Sakhalin again and took the position of Chairman of Seismological Council of the USSR Academy of Sciences. His work during this period was connected with automation of seismological observations in the USSR territory for the Academy of Science, and included initiation of the program for detailed estimation of seismic risk in earthquake-prone zones of the USSR. Unfortunately, disagreement with the leadership of the Institute of Physics of the Earth on the strategy and scientific policy in the problem of earthquake prediction resulted in his retirement from this position. Thus, in 1978, he moved to the Institute of Oceanology where he led the Institute's program of ocean bottom seismology. He had gained experience in this field when in Sakhalin, where the first work on the development and construction of ocean bottom seismographs (OBS) started in the 1970's. Several new types of the OBS's were developed and manufactured at the Institute's design bureau in Gelengic on the Black Sea. Professor Soloviev participated in several cruises of the research vessel "Dmitriy Mendeleev" in the Mediterranean and the Atlantic where the new OBS's were successfully deployed. Results of his work for this period were summarized in the book "History and the Perspectives of Sea Seismology", published in Moscow in 1985. Despite the fact that ocean bottom seismology became the primary part of his official work in the Academy of Sciences, Professor Soloviev continued his active participation in coordination of tsunami research and investigation in the Soviet Union and encouraged greater international cooperation. Since 1971 he was the permanent Chairman of the Tsunami Commission of the USSR Academy of Sciences and his leadership in this field was recognized by all his colleagues. He always paid special attention to the involvement of young scientists and worked to attract the attention of specialists from other fields to the tsunami problem. Professor Soloviev died on March 9, 1994 at the age 63 from cerebral thrombosis while he was working in his Moscow apartment, editing his second book on ocean bottom observations.



PROFESSOR SERGEI SOLOVIEV

1930 - 1984

TSUNAMI 1996

Marking the 50th anniversary of the 1946 tsunami at Hilo, which led to the present Pacific-wide warning system, increased tsunami research, and the Centennial of the great Sanriku earthquake and tsunami in Japan.

"Those who can not remember history are condemned to repeat it"
– Santana

An educational and awareness conference is planned for Hilo for April 1-2, 1996. We will review the lessons learned, the progress we have made, the things still to be accomplished, and priorities needed for tsunami and similar hazard mitigation. An open house and tour of the Pacific Tsunami Warning Center on Oahu will be available the following day.

The organizing committee consists of:

Co-Chairman
Jim Lander, University of Colorado CIRES
National Geophysical Data Center, NOAA,
Boulder, Colorado

Co-Chairman
George Curtis, University of Hawaii, Hilo and
Joint Institute for Marine and Atmospheric
Research, U.H. Manoa

- Walter Dudley, University of Hawaii, Hilo, and Hilo Tsunami Museum
- Harry Kim, Hawaii County Civil Defense, Hilo
- Don Gransback, Hawaii State Civil Defense, Honolulu
- Nobuo Shuto, Tohoku Univ, Tokyo
- Dennis Segrist, International Tsunami Information Center, Honolulu
- Augustine Furumoto, Hawaii Institute of Geophysics, University of Hawaii, Manoa

An advisory board will aid in planning and arranging support and coordination for the event among the organizations and countries involved:

- Fred Camfield, Corps of Engineers
- Mike Blackford, PTWC
- Eddie Bernard, NOAA/PMEL
- Yoshi Tsuji, Japan Earthquake Research Institute
- Paul Whitmore, Alaska Warning Center
- Roy Price, Hawaii Civil Defense
- Tad Murty, Australia Coastal Research
- Shigenobu Tanaka, Public works Research Institute, Asahi

Cooperating Organizations include:

- The Tsunami Society
- The International Tsunami Information Center
- The Joint Institute for Marine and Atmospheric Research, University of Hawaii
- The Hilo Tsunami Museum



*The Big Island
of
Hawaii*

April 1, 1996

APPLICATION FOR MEMBERSHIP

THE TSUNAMI SOCIETY
P.O. Box 8523
Honolulu, Hawaii 96815, USA

I desire admission into the Tsunami Society as: (Check appropriate box.)

Student

Member

Institutional Member

Name _____ Signature _____

Address _____ Phone No. _____

Zip Code _____ Country _____

Employed by _____

Address _____

Title of your position _____

FEE: Student \$5.00 Member \$25.00 Institution \$100.00

Fee includes a subscription to the society journal: SCIENCE OF TSUNAMI HAZARDS.

Send dues for one year with application. Membership shall date from 1 January of the year in which the applicant joins. Membership of an applicant applying on or after October 1 will begin with 1 January of the succeeding calendar year and his first dues payment will be applied to that year.

